CHALMERS
UNIVERSITY OF TECHNOLOGY

Simulation Model Development of Electric Motor and Controller

Master's thesis in Systems, Control and Mechatronics

Wang Han

Department of Electrical Engineering
CHALMERS UNIVERSITY OF TECHNOLOGY
Gothenburg, Sweden 2017

Simulation Model Development of Electric Motor and Controller

Thesis for the Degree of Master of Science in Engineering

Wang Han

Simulation Model Development of Electric Motor and Controller
Thesis for the Degree of Master of Science in Engineering
Wang Han

Supervisor: Michael Palander, CEVT
Examiner: Jonas Fredriksson, Department of Electrical Engineering

Cover: "GEELY EMGRAND EV " from CEVT

Simulation Model Development of Electric Motor and Controller
Thesis for the Degree of Master of Science in Engineering
Wang Han
Department of Electrical Engineering
Chalmers University of Technology

Abstract

As a result of the high efficiency requirement and the limited battery's capacity, the permanent magnent synchronous machine(PMSM) has become a popular alternative for electric motor drive system, especially for the plug-in hybrid electric vehicle(PHEV) in automotive applications. In this thesis, the salient PMSM is studied. A mathematical model of PMSM is derived from abc three-phase coordinates to dq rotating reference frame. The flux linkage, voltage and current equations which are used to analyze the performance of PMSMs are described both in equation form and matrix form. A Field oriented contro method is adopted for the speed control of the PMSM and a current regulator is designed using a method called Internal Model Control (IMC). The entire PMSM drive system, including plant model, current regulator, speed controller, sinusoidal pulse width modulation (SPWM) and inverter is designed, implemented and simulated using Matlab/Simulink software. The plant model of the PMSM and the motor control unit are also exported and included in CarMaker for complete vehicle verification. The simulation results are presented and a good dynamic response is shown.

Acknowledgements

Initially, I would like to thank my supervisor Michael Palander for giving me such a superb opportunity to conduct my master thesis at CEVT. His caring, encouragement and guidance have been crucial throughout the project.

I also want to express my gratitude to my examiner Jonas Fredriksson for his great support and academic experience. His valuable ideas and comments are gratefully appreciated.

I am very grateful to my good friend Muddassar Zahid Piracha, CEVT specialist also a Ph.D student at Chalmers, who provided me with great technical supprot from begining to the end. I would also like to thank Johan Hellsing, the expert at CEVT, who had helped me concerning technical issues at all times.

I appreciated all the people who have ever helped me. Without your help and support, I cannot successfully accomplish my master thesis.

Last but not least, I would love to thank my parents for their endless love and support. Because of them, my dream has come true. Love you now and forever!

Wang Han

Göteborg, August 2017

Contents

Contents

List of Figures

List of Tables

1

Introduction

In this first chapter, a brief introduction regarding the development of PHEVs (plug-in hybrid electric vehicles) is reviewed. The focus is put on electric motors and specifically PMSM (Permanent Magnet Synchronous Machine) which is broadly utilized in automotive industry. The objectives and outline of the thesis are also presented.

1.1   Development of PHEVs

In recent years, many countries across the world have been exploring and developing green vehicles since the petrol crisis and environmental problems throughout the world are becoming more and more severe. Consequently, electric vehicles, a vehicle of zero pollution, becomes a wise choice in these countries.

However, due to the cost of high-efficient batteries and the limited number of charging stations, Battery Electric Vehicles (BEVs) have not been widely applied into automotive market in many developing countries. Thus a more suitable vehicle, the Plug-in Hybrid Electric Vehicle (PHEV) is a better option in comparison with the BEV.

A PHEV is a hybrid vehicle which adopts rechargeable batteries that can be recharged by plugging it into external electrical outlets. A PHEV has an electric motor and an internal combustion engine (ICE). PHEVs are expected to consume less petroleum, lessen carbon dioxide emissions, counteract global warming, and be conducive to nations' energy independence, see [1].

A number of universities and corporations have promoted PHEVs as a method to realize the benefits of electric vehicles without the range limitation. However, due to the technical barriers and high development cost of batteries, the manufacturing of PHEVs still has a long way to go. Since the public awareness of environment is gradually increasing, the development of PHEVs is undoubtedly a tendency in the near future.

1.1.1 Powertrain Configuration

Plug-in hybrid electric vehicles have been already commercially launched into car market. Figure 1.1 illustrate a plug-in parallel-hybrid electric vehicles configuration.
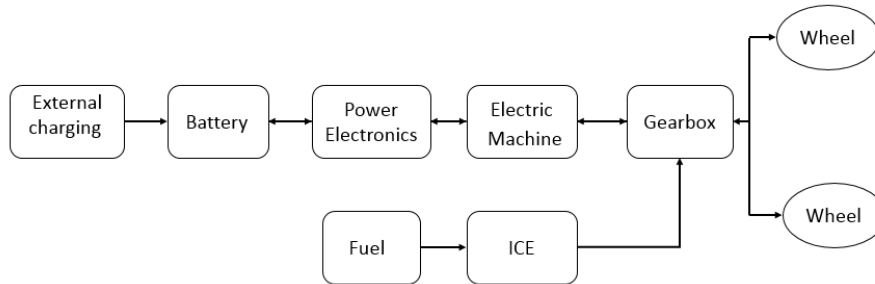
Figure 1.1: Parallel-Hybrid Electric Vehicles. The arrows represent directions of energy flow

In a parallel-hybrid electric vehicle, the propulsion power can be supplied by the ICE (internal combustion engine) alone, by the electric machine alone, or by a combination of both. Each energy source is connected to the driveshaft. Figure 1.1 also shows the energy flow direction. In the electric power supply, the battery can not only charged by external charging but also by recycling the energy when vehicle is braking, driving downhill and in the idle speed. Apparently, having a larger battery with external charging can increase the electric range.

1.1.2 Permanent Magnet Synchronous Machine

The electric drive system is one of the key component of a PHEV. The electric drive system can largely effect the performance of the vehicle. For the current development of the motor, the crucial parts of the technical upgrade are to improve its reliability and life expectancy.

Due to the restrictions of space and environment, the PMSM drive system applied in PHEVs has some advantages compared to the conventional electric drive system, such as higher efficiency in steady-state and operate constantly at synchronous speed. PMSMs also have the advantages of high power density, high power factor and is easy to maintain, see [2]. Therefore, PMSMs have become one of the significant development direction of electric motor in automotive applications.

1.2 Objectives of Thesis

The goal of this thesis is to design and implement a simulation model of a PMSM and its controller to accomplish an electric drive system for PHEVs.

The aim of this thesis is to simulate the complete electric drive system in a virtual surrounding so as to shorten development time and save cost. It can also provide a better basis for decisions regarding requirement setting and dimensioning.

The modeling of the PMSM and its controller is designed and implemented in Matlab/Simulink.

1.3 Outline of Thesis

The chapters are outlined below.

Chapter 2 presents the mathematical model of PMSM. FOC method and IMC method for controller design are introduced in detail.

chapter 3 reviews the basic principles of SPWM and inverter.

Chapter 4 demonstrates the simulation results and related analysis.

Chapter 5 focuses on the implementation of the plant model of PMSM and its controller in CarMaker.

Chapter 6 summarizes the conclusions of the work and brings up some interesting problems which can be used for future research.

2

Dynamical Modelling of PMSMs

In order to design and develop control schemes for a PMSM drive system, the dynamic model of a PMSM depending upon control would be necessary. The dynamic model may vary whey using them to design control and simulation algorithms of a PMSM, see[3].

It is well-known that the performance of a three-phase PMSM is described by the voltage and inductance equations, see[4]. Conventionally, a two-phase equivalent circuit model instead of a complicated three-phase model has been adopted to analyze reluctance synchronous machine. The theory is now applied in the analysis of different kinds of motors including PMSMs, induction motors etc, see[5]. The two-phase(d-q) equivalent circuit model is able to effectively analyze a PMSM since it reduces the complexity of these differential equations as mentioned in [6].

In this chapter, the dynamical modelling and analysis of a PMSM are described. Based on well-known Clarke and Park transformation, the three-phase model of a PMSM is transformed to $\alpha - \beta$ stationary model in the first place, and then $\alpha - \beta$ stationary model is transformed to an equivalent two-phase(d-q) rotating model. Using these transformations, many properties of a PMSM can be studied without complexities in the voltage equations, see[4].

Throughout the derivation of d-q mathematical model of a PMSM, the following assumptions are made [7]:

- Stator windings produce sinusoidal MMF distribution. Space harmonics in the air-gap are neglected.

- There is no zero-component in the three-phase quantities.

- Balanced three-phase sinusoidal supply voltage is considered.

- Eddy current and hysteresis effects are neglected

- Iron losses are neglected.

- Resistances are independent of temperature and frequency.

2.1   Mathematical Model of a PMSM

According to [3], based on different rotor constructions, there are two major varieties of PMSMs: namely interior PMSMs (with saliency) and surface-mounted PMSMs (without saliency). The main difference is that the inductance in an interior PMSM vary as a function of rotor angle, however a surface-mounted PMSM has quite a fixed inductance for any rotor angle as mentioned in [8].

In automotive applications, a salient PMSM is a preference since it is easy to have sensorless control in case of sensor failure. Thus in this section, the mathematical model of a PMSM with saliency is developed in detail.

A PMSM with more than one pole-pairs has stator windings comprising a corresponding multiple set of coils. For the purpose of analysis, it is convenient to consider only a single pole-pair and recognize that conditions associated with other pole-pairs are identical to the conditons for only one pole-pair, see[9].

Figure 2.1 illustrates a schematic diagram of a cross section of a three-phase PMSM along with $\alpha - \beta$ reference frame.
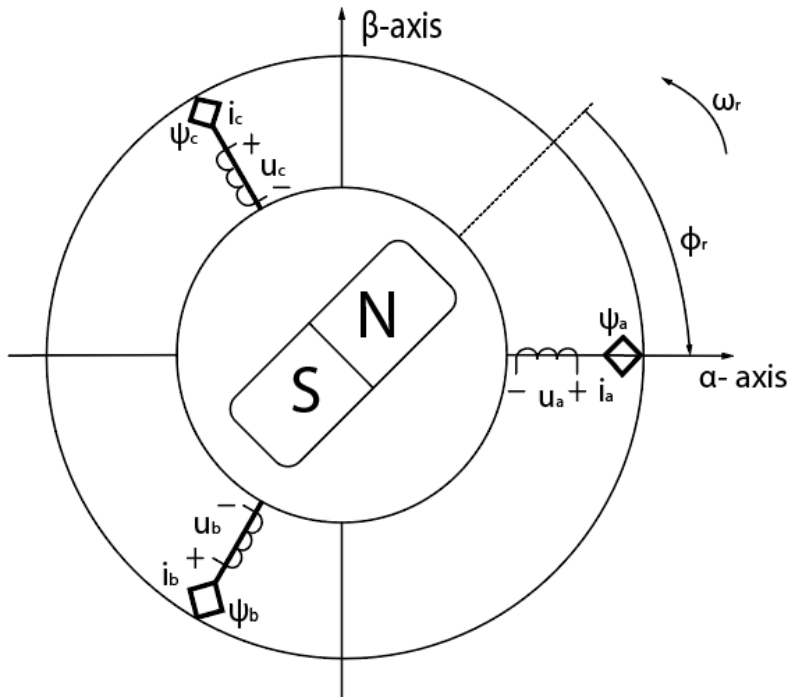
Figure 2.1: View of a three-phase PMSM.

Note that three-phases stator windings are displaced 120° electrical degrees apart in space. As shown in Figure 2.1 that i_a, i_b, i_c are the currents of the stator a-phase, b-phase, c-phase respectively, u_a, u_b, u_c are the voltages of the stator a-phase, b-phase, c-phase respectively, ψ_a, ψ_b, ψ_c are the flux linkages of the stator a-phase, b-phase, c-phase respectively. The α-axis and β-axis are orthogonal. ϕ_r is electrical rotor

angle.

The stator flux linkages for three-phase model are given by:

$$
\begin{aligned}
\psi_a &= L_{aa}i_a + L_{ab}i_b + L_{ac}i_c + \Psi_m cos(\phi_r) \\
\psi_b &= L_{ba}i_a + L_{bb}i_b + L_{bc}i_c + \Psi_m cos(\phi_r - \frac{2\pi}{3}) \\
\psi_c &= L_{ca}i_a + L_{cb}i_b + L_{cc}i_c + \Psi_m cos(\phi_r + \frac{2\pi}{3})
\end{aligned}
\tag{2.1}
$$

where L_{aa}, L_{bb}, L_{cc} are the self-inductances of the stator a-phase, b-phase, c-phase respectively.

$L_{ab} = L_{ba}, L_{bc} = L_{cb}, L_{ca} = L_{ac}$ are the mutual inductances between a-phase and b-phase, b-phase and c-phase, c-phase and a-phase respectively.

Ψ_m is the flux linkage established by the permanent magnent.

In the flux linkage equations, inductances are the functions of the rotor angle ϕ_r. Due to saliency, the self-inductance of the stator windings can be approximately expressed as:

$$
\begin{aligned}
L_{aa} &= L_{ls} + L_{0s} - L_{ss}cos(2\phi_r) \\
L_{bb} &= L_{ls} + L_{0s} - L_{ss}cos(2(\phi_r - \frac{2\pi}{3})) \\
L_{cc} &= L_{ls} + L_{0s} - L_{ss}cos(2(\phi_r + \frac{2\pi}{3}))
\end{aligned}
\tag{2.2}
$$

where L_{ls} is the leakage inductance of the stator winding, L_{0s} is the average inductance due to space fundamental air-gap flux as mentioned in [6], L_{ss} is the inductance fluctuation due to saliency.

The mutual inductances between the stator windings can be described as:

$$
\begin{aligned}
L_{ab} = L_{ba} &= -\frac{1}{2}L_{0s} - L_{ss}cos(2(\phi_r - \frac{\pi}{3})) \\
L_{bc} = L_{cb} &= -\frac{1}{2}L_{0s} - L_{ss}cos(2(\phi_r + \pi)) \\
L_{ca} = L_{ac} &= -\frac{1}{2}L_{0s} - L_{ss}cos(2(\phi_r + \frac{\pi}{3}))
\end{aligned}
\tag{2.3}
$$

Assuming there is no zero-component in the three-phase quantities, the three-phase

flux linkages can be expressed in this way:

$$\psi_a = (L_{ls} + \frac{3}{2}L_{0s} - \frac{3}{2}L_{ss}cos(2\phi_r))i_a + \frac{\sqrt{3}}{2}L_{ss}sin(2\phi_r)(i_c - i_b) + \Psi_m cos(\phi_r)$$

$$\psi_b = (L_{aa0} + \frac{3}{2}L_{0s} - \frac{3}{2}L_{ss}cos(2(\phi_r - \frac{2\pi}{3})))i_b + \frac{\sqrt{3}}{2}L_{ss}sin(2(\phi_r - \frac{2\pi}{3}))(i_a - i_c)$$
$$+ \Psi_m cos(\phi_r - \frac{2\pi}{3})$$

$$\psi_c = (L_{aa0} + \frac{3}{2}L_{0s} - \frac{3}{2}L_{ss}cos(2(\phi_r + \frac{2\pi}{3})))i_c + \frac{\sqrt{3}}{2}L_{ss}sin(2(\phi_r + \frac{2\pi}{3}))(i_b - i_a)$$
$$+ \Psi_m cos(\phi_r + \frac{2\pi}{3})$$

$$(2.4)$$

For the coupled-circuit, the three-phase stator voltages can be expressed as:

$$u_a = R_a i_a + \frac{d\psi_a}{dt}$$
$$u_b = R_b i_b + \frac{d\psi_b}{dt} \qquad (2.5)$$
$$u_c = R_c i_c + \frac{d\psi_c}{dt}$$

where R_a, R_b, R_c are the resistances of the stator a-phase, b-phase, c-phase respectively. $R_a = R_b = R_c = R_s$ is assumed under amplitude invariant transformation.

The zero sequence is neglected and the amplitude invariant transformation is used, then the stator voltage equation from three phase to α-β stationary reference frame is expressed by:

$$\underline{u}_s^s = u_{s\alpha} + ju_{s\beta} = \frac{2}{3}(u_a + u_b e^{j\frac{2\pi}{3}} + u_c e^{j\frac{4\pi}{3}})$$
$$= \frac{2}{3}(R_a i_a + \frac{d\psi_a}{dt} + (R_b i_b + \frac{d\psi_b}{dt})e^{j\frac{2\pi}{3}} + (R_c i_c + \frac{d\psi_c}{dt})e^{j\frac{4\pi}{3}}) \qquad (2.6)$$
$$= R_s \frac{2}{3}(i_a + i_b e^{j\frac{2\pi}{3}} + i_c e^{j\frac{4\pi}{3}}) + \frac{d}{dt}(\frac{2}{3}(\psi_a + \psi_b e^{j\frac{2\pi}{3}} + \psi_c e^{j\frac{4\pi}{3}}))$$

$\underline{u}_s^s$ can be simplified to be given as:

$$\underline{u}_s^s = R_s \underline{i}_s^s + \frac{d\underline{\psi}_s^s}{dt} \qquad (2.7)$$

where $\underline{u}_s^s, \underline{i}_s^s, \underline{\psi}_s^s$ are space vector of the three-phase stator voltages, currents and flux linkages respectively, which are all described in α-β stationary reference frame.

Based on the equation above, the current in α-β model is definded as:

$$\underline{i}_s^s = i_{s\alpha} + ji_{s\beta} = \frac{2}{3}(i_a + i_b e^{j\frac{2\pi}{3}} + i_c e^{j\frac{4\pi}{3}}) \qquad (2.8)$$

Similarly, the flux linkage in α-β model is defined as:

$$\underline{\psi}_s^s = \psi_{s\alpha} + j\psi_{s\beta} = \frac{2}{3}(\psi_a + \psi_b e^{j\frac{2\pi}{3}} + \psi_b e^{j\frac{4\pi}{3}}) \tag{2.9}$$

The resultant voltage, current, and flux linkage space vectors shown in equations (2.7),(2.8),(2.9) for the stator are calculated by multiplying instantaneous phase values by the stator winding orientations in which the stator a-phase direction is chosen to the direction of maximum MMF, b-phase, c-phase are 120°(electrical degree) ahead of the a-phase respectively, see[6].

In order to calculate the flux linkage $\underline{\psi}_s^s$, the three-phase flux linkages can be expressed in a different way:

$$\psi_a = (L_{ls} + \frac{3}{2}L_{0s})i_a + \frac{3}{2}L_{ss}cos(2\phi_r)i_a + \frac{\sqrt{3}}{2}L_{aa2}sin(2\phi_r)(i_c - i_b) + \Psi_m cos(\phi_r)$$

$$\psi_b = (L_{ls} + \frac{3}{2}L_{0s})i_b + \frac{3}{2}L_{ss}cos(2(\phi_r - \frac{2\pi}{3}))i_b + \frac{\sqrt{3}}{2}L_{aa2}sin(2(\phi_r - \frac{2\pi}{3}))(i_a - i_c)$$

$$+ \Psi_m cos(\phi_r - \frac{2\pi}{3})$$

$$\psi_c = (L_{ls} + \frac{3}{2}L_{0s})i_c + \frac{3}{2}L_{ss}cos(2(\phi_r + \frac{2\pi}{3}))i_c + \frac{\sqrt{3}}{2}L_{aa2}sin(2(\phi_r + \frac{2\pi}{3}))(i_b - i_a)$$

$$+ \Psi_m cos(\phi_r + \frac{2\pi}{3}) \tag{2.10}$$

The transformation of the stator flux linkage can be described by splitting the flux equations above into 4 parts and taking one at the time. Thus, the new four flux linkages equations are as follows: (superscirpt "*" indicates complex conjugate):

$$\underline{\psi}_{s,1}^s = \frac{2}{3}((L_{ls} + \frac{3}{2}L_{0s})i_a + (L_{ls} + \frac{3}{2}L_{0s})i_b e^{j\frac{2\pi}{3}} + (L_{ls} + \frac{3}{2}L_{0s})i_c e^{j\frac{4\pi}{3}}) = (L_{ls} + \frac{3}{2}L_{0s})\underline{i}_s^s$$

$$\underline{\psi}_{s,2}^s = \frac{2}{3}(\frac{3}{2}L_{ss}cos(2\phi_r)i_a + \frac{3}{2}L_{ss}cos(2(\phi_r - \frac{2\pi}{3}))i_b e^{j\frac{2\pi}{3}} + \frac{3}{2}L_{ss}cos(2(\phi_r + \frac{2\pi}{3}))i_c e^{j\frac{4\pi}{3}})$$

$$= \frac{3}{4}L_{ss}e^{j2\phi_r}\frac{2}{3}(i_a + i_b e^{-j\frac{2\pi}{3}} + i_c e^{j\frac{2\pi}{3}}) = \frac{3}{4}L_{ss}e^{j2\phi_r}\underline{i}_s^{s*}$$

$$\underline{\psi}_{s,3}^s = \frac{2}{3}(\frac{\sqrt{3}}{2}L_{ss}sin(2\phi_r)(i_c - i_b) + \frac{\sqrt{3}}{2}L_{ss}sin(2(\phi_r - \frac{2\pi}{3}))(i_a - i_c)e^{j\frac{2\pi}{3}} + \frac{\sqrt{3}}{2}L_{ss}$$

$$sin(2(\phi_r + \frac{2\pi}{3}))(i_b - i_a)e^{j\frac{4\pi}{3}}) = L_{ss}e^{j2\phi_r}\frac{\sqrt{3}}{2}\frac{e^{j\frac{2\pi}{3}} - e^{-j\frac{2\pi}{3}}}{2j}\underline{i}_s^{s*} = \frac{3}{4}L_{ss}e^{j2\phi_r}\underline{i}_s^{s*}$$

$$\underline{\psi}_{s,4}^s = \frac{2}{3}(\Psi_m cos\phi_r + \Psi_m cos(\phi_r - \frac{2\pi}{3})e^{j\frac{2\pi}{3}} + \Psi_m cos(\phi_r + \frac{2\pi}{3})e^{j\frac{4\pi}{3}}) = \Psi_m e^{j\phi_r} \tag{2.11}$$

The flux linkage $\underline{\psi}_s^s$ is the sum of $\underline{\psi}_{s,1}^s, \underline{\psi}_{s,2}^s, \underline{\psi}_{s,3}^s, \underline{\psi}_{s,4}^s$:

$$\underline{\psi}_s^s = \underline{\psi}_{s,1}^s + \underline{\psi}_{s,2}^s + \underline{\psi}_{s,3}^s + \underline{\psi}_{s,4}^s = (L_{ls} + \frac{3}{2}L_{0s})\underline{i}_s^s + \frac{3}{2}L_{ss}e^{j2\phi_r}\underline{i}_s^{s*} + \Psi_m e^{j\phi_r} \tag{2.12}$$

By combining the first and second term of equation(2.12), the total flux linkage is given as:

$$\underline{\psi}_s^s = \underline{L}_s \underline{i}_s^s + \Psi_m e^{j\phi_r} \tag{2.13}$$

where $\underline{L}_s$ is leakage and mutual inductance.

Now, the three-phase stator voltages, currents and flux linkages are all described in α-β stationary reference frame. Multiplying the quantities with $e^{-j\theta}$ will transform α-β stationary reference frame to d-q rotating reference frame. This leads to the voltages, currents, flux linkages and inductance equations having time-invariant coefficients, see[6].

Figure 2.2 illustrates the coordinate transformation from $\alpha - \beta$ stationary reference frame to d-q rotating frame.
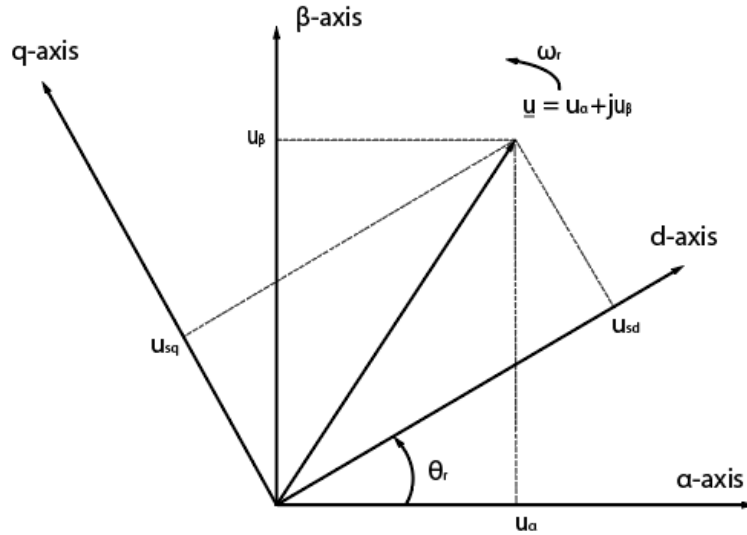
Figure 2.2: Coordinate transformation from $\alpha - \beta$ frame to d-q frame

Note that θ_r is d-q transformation angle.

As shown in Figure 2.2,the coordinate transformation calculation is as follows:

$$
\begin{aligned}
\underline{u}_s = \underline{u}_s^s e^{-j\theta_r} &= (u_{s\alpha} + ju_{s\beta})(cos\theta_r - jsin\theta_r) \\
&= (u_{s\alpha}cos\theta_r + u_{s\beta}sin\theta_r) + j(u_{s\beta}cos\theta_r - u_{s\alpha}sin\theta_r) \\
&= u_{sd} + ju_{sq}
\end{aligned} \tag{2.14}
$$

The transformation can also be expressed in matrix form:

$$
\begin{bmatrix} u_{sd} \\ u_{sq} \end{bmatrix} = \begin{bmatrix} cos\theta_r & sin\theta_r \\ -sin\theta_r & cos\theta_r \end{bmatrix} \begin{bmatrix} u_{s\alpha} \\ u_{s\beta} \end{bmatrix} \tag{2.15}
$$

Based on transformation rule above, the relations between α-β stationary reference frame and d-q rotating reference frame regarding current, voltage and flux linkage are presented respectively as :

$$\underline{i}_s = \underline{i}_s^s e^{-j\theta_r} \tag{2.16}$$

$$u_s = \underline{u}_s^s e^{-j\theta_r} \tag{2.17}$$

$$\underline{\psi}_s = \underline{\psi}_s^s e^{-j\theta_r} \tag{2.18}$$

According to equation(2.17), the stator voltage equation (2.7) in α-β stationary coordinates is expressed as:

$$\underline{u}_s^s = \underline{u}_s e^{j\theta_r} = R_s \underline{i}_s e^{j\theta_r} + \frac{d}{dt}(\underline{\psi}_s e^{j\theta_r}) = R_s \underline{i}_s e^{j\theta_r} + \frac{d\underline{\psi}_s}{dt}e^{j\theta_r} + j\omega_r \underline{\psi}_s e^{j\theta_r} \tag{2.19}$$

where $\omega_r = \frac{d\theta_r}{dt}$ is the electrical rotor speed

Therefore the voltage equation in d-q rotating coordinates is given by:

$$\underline{u}_s = R_s \underline{i}_s + \frac{d\underline{\psi}_s}{dt} + j\omega_r \underline{\psi}_s \tag{2.20}$$

Likewise, based on equation (2.18), flux linkage equation (2.12) in α-β stationary coordinates is expressed as:

$$\underline{\psi}_s^s = \underline{\psi}_s e^{j\theta_r} = (L_{ls} + \frac{3}{2}L_{0s})\underline{i}_s e^{j\theta_r} + \frac{3}{2}L_{ss}e^{j2\phi_r}(\underline{i}_s e^{j\theta_r})^* + \Psi_m e^{j\phi_r} \tag{2.21}$$

Flux linkage$\underline{\psi}_s$ in d-q rotating coordinates is thus given by:

$$\underline{\psi}_s = (L_{ls} + \frac{3}{2}L_{0s})\underline{i}_s + \frac{3}{2}L_{ss}e^{j(2\phi_r - 2\theta_r)}\underline{i}_s^* + \Psi_m e^{j(\phi_r - \theta_r)} \tag{2.22}$$

Perfect field field orientation is implemented in this thesis, therefore electric rotor angle is equal to the d-q transformation angle, $\theta_r = \phi_r$.

Hence the flux linkage $\underline{\psi}_s$ is

$$\underline{\psi}_s = (L_{ls} + \frac{3}{2}L_{0s})\underline{i}_s + \frac{3}{2}L_{ss}\underline{i}_s^* + \Psi_m \tag{2.23}$$

Now, the current and volatege are described in d-q coordinates, then $\underline{i}_s$, $\underline{i}_s^*$, $\underline{u}_s$ can be simply respectively defined as

$$\underline{i}_s = i_{sd} + ji_{sq} \tag{2.24}$$

$$\underline{i}_s^* = i_{sd} - ji_{sq} \tag{2.25}$$

$$\underline{u}_s = u_{sd} + ju_{sq} \tag{2.26}$$

Flux linkage $\underline{\psi}_s$ can be further expressed as:

$$\begin{aligned}\underline{\psi}_s &= (L_{ls} + \frac{3}{2}L_{0s} + \frac{3}{2}L_{ss})\underline{i}_{sd} + j(L_{ls} + \frac{3}{2}L_{0s} - \frac{3}{2}L_{ss})\underline{i}_{sq} + \Psi_m \\ &= L_{sd}\underline{i}_{sd} + jL_{sq}\underline{i}_{sq} + \Psi_m\end{aligned} \tag{2.27}$$

where L_{sd}, L_{sq} can be named as the stator inductance in d coordinate and q coordinate respectively. Expanding stator voltage equation (2.20) based on equations (2.24),(2.26)and final flux linkage equation (2.27), then voltage equations in d-q rotating coordinates are given by:

$$u_{sd} = R_s i_{sd} + L_{sd}\frac{di_{sd}}{dt} - \omega_r L_{sq} i_{sq} \tag{2.28}$$

$$u_{sq} = R_s i_{sq} + L_{sq}\frac{di_{sq}}{dt} + \omega_r L_{sd} i_{sd} + \omega_r \Psi_m \tag{2.29}$$

From the well-known relation power $P = R_e\{\underline{U}\underline{I}^*\}$, for single-phase rms-value-scaled phasors $\underline{U}$ and $\underline{I}$, it may be conjectured that the instantaneous power in a three-phase system is proportional to [10]:

$$R_e\{\underline{u}_s^s \underline{i}_s^{s^*}\} = R_e\{\underline{u}_s e^{j\theta_r}(\underline{i}_s e^{j\theta_r})^*\} = R_e\{\underline{u}_s \underline{i}_s^*\} \tag{2.30}$$

From the space-vector definition,

$$\underline{u}_s^s \underline{i}_s^{s^*} = (\frac{2K}{3})^2(u_a + u_b e^{j\frac{2\pi}{3}} + u_c e^{j\frac{4\pi}{3}})(i_a + i_b e^{j\frac{2\pi}{3}} + i_c e^{j\frac{4\pi}{3}})^* \tag{2.31}$$

Assuming that $i_a + i_b + i_c = 0$ and observing that $e^{j\frac{4\pi}{3}} = e^{-j\frac{2\pi}{3}}$, the

$$\underline{u}_s^s \underline{i}_s^{s^*} = (\frac{2K}{3})^2(u_a i_a + u_b i_b + u_c i_c) \tag{2.32}$$

So the instantaneous power is given by

$$P = \frac{3}{2K^2}R_e\{\underline{u}_s^s \underline{i}_s^{s^*}\} = \frac{3}{2K^2}R_e\{\underline{u}_s \underline{i}_s^*\} = u_a i_a + u_b i_b + u_c i_c \tag{2.33}$$

Thus the electric power to the shaft can be calculated as by following the equation (2.33)

$$P_e = \frac{3}{2K^2}R_e\{j\omega_r \underline{\psi}_s \underline{i}_s^*\} \tag{2.34}$$

Since for a complex number $z = x + jy$, the $[R_e\{j\underline{z}\} = R_e j(x+jy) = -y = -I_m\{\underline{z}\}]$, see[10],thus the

$$P_e = -\frac{3\omega_r}{2K^2}I_m\{\underline{\psi}_s \underline{i}_s^*\} = \frac{3\omega_r}{2K^2}I_m\{\underline{\psi}_s^* \underline{i}_s\} \tag{2.35}$$

The power can be expressed as:

$$P_e = T_e \Omega_r \tag{2.36}$$

where T_e is electrical torque, Ω_r is mechanical rotor speed.

Mechanical rotor speed is expressed as:

$$\Omega_r = \frac{\omega_r}{n_p} \tag{2.37}$$

where ω_r is electrical rotor speed, n_p is the number of pole pairs ,

Thus the following relation for the electrical torque is obtained:

$$
\begin{aligned}
T_e &= \frac{P_e}{\Omega_r} = \frac{n_p P_e}{\omega_r} = \frac{3\omega_r n_p}{2\omega_r K^2} I_m\{\underline{\psi}_s^* \underline{i}_s\} \\
&= \frac{3n_p}{2K^2} I_m\{(L_{sd} i_{sd} + jL_{sq} i_{sq} + \Psi_m)^* \underline{i}_s\} \\
&= \frac{3n_p}{2K^2} I_m\{(L_{sd} i_{sd} - jL_{sq} i_{sq})(i_{sd} + ji_{sq}) + \Psi_m \underline{i}_s\} \\
&= \frac{3n_p}{2K^2}(L_{sd} i_{sd} i_{sq} - L_{sq} i_{sq} i_{sd} + \Psi_m i_{sq})
\end{aligned}
\tag{2.38}
$$

Thus, the electrical torque is:

$$
T_e = \frac{3n_p}{2K^2}((L_{sd} - L_{sq})i_{sq} i_{sd} + \Psi_m i_{sq}) \tag{2.39}
$$

The relation between electrical torque and load torque is given by

$$
J\frac{d\Omega_r}{dt} = \frac{J}{n_p}\frac{d\omega_r}{dt} = T_e - T_L \tag{2.40}
$$

where J is inertia of the motor. The complete load torque T_L should consist of two parts, one is a speed independent part determined by the viscous cofficient B, another one is direct extra load torque input $T_{L,extra}$.

$$
T_L = B\Omega_r + T_{L,extra} = \frac{B\omega_r}{n_p} + T_{L,extra} \tag{2.41}
$$

Mechanical rotor position is given by:

$$
\Phi_r = \frac{\phi_r}{n_p} \tag{2.42}
$$

where ϕ_r is electric rotor position which is equal to the d-q transformation angle θ_r

The electrical rotor speed can be calculated by electric rotor position

$$
\omega_r = \frac{d\phi_r}{dt} \tag{2.43}
$$

2.2 Clarke's and Park's Transformation

This section reviews the principle of Clarke's and Park's Transformation. Actually, the theory of both transformation methods has been utilized last section when building the mathematical model of a PMSM. In this section, the method will be simply described in a more straightforward way, the voltages, currents and flux linkages are based on matrix form and related calculations are also conducted in matrix form.

As mentioned last section, according to [4], the transformation of stationary circuits to a stationary reference frame with two-phase variables α and β was developed by Clarke. And Park's transformation with two-phase variables d and q has the unique property of eliminating all time varying inductances from the three-phase voltage equations due to the rotor spinning.

For Clarke Transformation, in order to make the transformation be invertible, the zero-consequence component is added as a third variable. The resulting transformation from a-b-c three-phase stationary frame to α-β reference frame is

$$\left[f_{\alpha\beta0} \right] = T_{\alpha\beta0} \left[f_{abc} \right] \tag{2.44}$$

where $\left[f_{\alpha\beta0} \right] = \begin{bmatrix} f_\alpha & f_\beta & f_0 \end{bmatrix}^T$ and $\left[f_{abc} \right] = \begin{bmatrix} f_a & f_b & f_c \end{bmatrix}^T$

f stands for voltage, current, flux linkage. The transformation matrix $T_{\alpha\beta0}$ is given by [4]:

$$T_{\alpha\beta0} = \frac{2}{3} \begin{bmatrix} 1 & -\frac{1}{2} & -\frac{1}{2} \\ 1 & \frac{\sqrt{3}}{2} & -\frac{\sqrt{3}}{2} \\ \frac{1}{2} & \frac{1}{2} & \frac{1}{2} \end{bmatrix} \tag{2.45}$$

The inverse transformation is given by

$$\left[f_{abc} \right] = T_{\alpha\beta0}^{-1} \left[f_{\alpha\beta0} \right] \tag{2.46}$$

where inverse transformation matrix is described by

$$T_{\alpha\beta0}^{-1} = \begin{bmatrix} 1 & 0 & 1 \\ -\frac{1}{2} & \frac{\sqrt{3}}{2} & 1 \\ -\frac{1}{2} & -\frac{\sqrt{3}}{2} & 1 \end{bmatrix} \tag{2.47}$$

For Park Transformation, a reference frame fixed on the rotor, i.e, dq frame is adopted. Thus the stator and rotor variables can be observed as constant values from the rotor point of view.

The transformation equation from three-phase stationary frame to $d - q$ reference frame is given by

$$\left[f_{dq0} \right] = T_{dq0} \left[f_{abc} \right] \tag{2.48}$$

where $\left[f_{dq0} \right] = \begin{bmatrix} f_d & f_q & f_0 \end{bmatrix}^T$ and $\left[f_{abc} \right] = \begin{bmatrix} f_a & f_b & f_c \end{bmatrix}^T$

Likewise, f stands for voltage, current, flux linkage. The dq0 transformation matrix is defined as [4]:

$$T_{dq0} = \frac{2}{3} \begin{bmatrix} cos\theta_r & cos(\theta_r - \frac{2\pi}{3}) & cos(\theta_r + \frac{2\pi}{3}) \\ -sin\theta_r & -sin(\theta_r - \frac{2\pi}{3}) & -sin(\theta_r + \frac{2\pi}{3}) \\ \frac{1}{2} & \frac{1}{2} & \frac{1}{2} \end{bmatrix} \tag{2.49}$$

The inverse transformation is given by

$$\left[f_{abc}\right] = T_{dq0}^{-1}\left[f_{dq0}\right] \tag{2.50}$$

where dq0 inverse transformation matrix is described by

$$T_{dq0}^{-1} = \frac{2}{3}\begin{bmatrix} cos\theta_r & -sin\theta_r & 1 \\ cos(\theta_r - \frac{2\pi}{3}) & -sin(\theta_r - \frac{2\pi}{3}) & 1 \\ cos(\theta_r + \frac{2\pi}{3}) & -sin(\theta_r + \frac{2\pi}{3}) & 1 \end{bmatrix} \tag{2.51}$$

From the last modelling section, based on the self-inductance equations (2.2) and mutual inductance (2.3), all stator inductances are represented in matrix form below:

$$L_{stator} = \begin{bmatrix} L_{aa} & L_{ab} & L_{ac} \\ L_{ba} & L_{bb} & L_{bc} \\ L_{ca} & L_{cb} & L_{cc} \end{bmatrix} \tag{2.52}$$

Due to the presence of permanent magnet on the rotor, the flux linkages in the stator windings are expressed as in matrix form :

$$\left[\psi_r\right] = \begin{bmatrix} \Psi_m cos(\phi_r) \\ \Psi_m cos(\phi_r - \frac{2\pi}{3}) \\ \Psi_m cos(\phi_r + \frac{2\pi}{3}) \end{bmatrix} = \begin{bmatrix} \psi_{ra} \\ \psi_{rb} \\ \psi_{rc} \end{bmatrix} \tag{2.53}$$

where ψ_{ra}, ψ_{rb}, ψ_{rc} are flux linkages established by permanent magnet in the stator a, b, c phase windings respectively.

Three-phase voltage equations can be rewritten as:

$$\left[u_s\right] = R_s\left[i_s\right] + \frac{d}{dt}\left[\psi_s\right] \tag{2.54}$$

where

$$\left[\psi_s\right] = \begin{bmatrix} \psi_a & \psi_b & \psi_c \end{bmatrix}^T \tag{2.55}$$

$$\left[u_s\right] = \begin{bmatrix} u_a & u_b & u_c \end{bmatrix}^T \tag{2.56}$$

$$\left[i_s\right] = \begin{bmatrix} i_a & i_b & i_c \end{bmatrix}^T \tag{2.57}$$

$\left[\psi_s\right], \left[u_s\right], \left[i_s\right]$ refer to the three-phase flux linkages, three-phase stator voltages and three-phase currents.

The matrix flux linkages of the three-phase stator windings can also be expressed as:

$$\left[\psi_s\right] = L_{stator}\left[i_s\right] + \left[\psi_r\right] \tag{2.58}$$

where L_{stator} is the stator inductance matrix varying with rotor angle. $\left[\psi_r\right]$ is the flux linkage matrix due to the permanent magnet.

Based on the original d-q Park's transformation matrix T_{dq0}, the three-phase flux linkages, three-phase stator voltages and three-phase currents can be transformed as:

$$\left[\psi_{dq0}\right] = \left[T_{dq0}\right]\left[\psi_s\right] \tag{2.59}$$

$$\left[u_{dq0}\right] = \left[T_{dq0}\right]\left[u_s\right] \tag{2.60}$$

$$\left[i_{dq0}\right] = \left[T_{dq0}\right]\left[i_s\right] \tag{2.61}$$

The matrix flux linkages in dq reference frame is obtained by:

$$\left[\psi_{dq0}\right] = \left[T_{dq0}\right]L_{stator}\left[T_{dq0}\right]^{-1}\left[i_{dq0}\right] + \left[T_{dq0}\right]\left[\psi_r\right] \tag{2.62}$$

where

$$\left[\psi_{dq0}\right] = \begin{bmatrix}\psi_{sd} & \psi_{sq} & \psi_0\end{bmatrix}^T \tag{2.63}$$

$$\left[i_{dq0}\right] = \begin{bmatrix}i_{sd} & i_{sq} & i_0\end{bmatrix}^T \tag{2.64}$$

The term $\left[T_{dq0}\right]L_{stator}\left[T_{dq0}\right]^{-1}$ is the transformation matrix which transforms the phase inductance matrix L_{stator} into the inductance matrix based on the dq reference frame $\left[L_{dq0}\right]$

$$\left[L_{dq0}\right] = \begin{bmatrix}L_{sd} & L_{sq} & L_0\end{bmatrix}^T \tag{2.65}$$

By simplifying the RHS of equation (2.62), the d-q axis flux linkages, ψ_{sd} and ψ_{sq}, the d-q axis inductances, L_{sd} and L_{sq}, d-q axis currents i_{sd}, i_{sq} are obtained as follows:

$$\psi_{sd} = (L_{ls} + \frac{3}{2}(L_{0s} + L_{ss}))i_{sd} + \Psi_m = L_{sd}i_{sd} + \Psi_m \tag{2.66}$$

$$\psi_{sq} = (L_{ls} + \frac{3}{2}(L_{0s} - L_{ss}))i_{sq} = L_{sq}i_{sq} \tag{2.67}$$

$$\psi_0 = L_{ls}i_0 \tag{2.68}$$

The next part is the derivation of the dq axis voltages.

If the equations (2.59), (2.60), (2.61) are substituted into (2.54), then the stator voltage equation is written in d-q coordinates as:

$$\left[u_{dq0}\right] = \left[T_{dq0}\right]R_s\left[T_{dq0}\right]^{-1}\left[i_{dq0}\right] + \left[T_{dq0}\right]\frac{d}{dt}(\left[T_{dq0}\right]^{-1}\left[\phi_{dqo}\right]) \tag{2.69}$$

where

$$\left[u_{dq0}\right] = \begin{bmatrix}u_{sd} & u_{sq} & u_0\end{bmatrix}^T \tag{2.70}$$

Since the resistance R_s is a scalar, the second term has a derivative part, the stator voltage equation can be further expressed as:

$$\left[u_{dq0}\right] = R_s\left[i_{dq0}\right] + \left[T_{dq0}\right]\left(\frac{d}{dt}\left(\left[T_{dq0}\right]^{-1}\right)\left[\phi_{dqo}\right] + \left[T_{dq0}\right]^{-1}\frac{d}{dt}\left[\phi_{dqo}\right]\right) \qquad (2.71)$$

Expanding the second term above equation, finally, the stator voltage equation in d-q coordinates is expressed as

$$\left[u_{dq0}\right] = R_s\left[i_{dq0}\right] + \left[T_{dq0}\right]\left(\frac{d}{dt}\left[T_{dq0}\right]^{-1}\right)\left[\phi_{dqo}\right] + \frac{d}{dt}\left[\phi_{dqo}\right] \qquad (2.72)$$

Taking the derivative of $\left[T_{dq0}\right]^{-1}$, i.e., equation (2.49),the matrix is

$$\frac{d}{dt}\left[T_{dq0}\right]^{-1} = \omega_r\begin{bmatrix} -sin\theta_r & -cos\theta_r & 0 \\ -sin(\theta_r - \frac{2\pi}{3}) & -cos(\theta_r - \frac{2\pi}{3}) & 0 \\ -sin(\theta_r + \frac{2\pi}{3}) & -cos(\theta_r + \frac{2\pi}{3}) & 0 \end{bmatrix} \qquad (2.73)$$

where ω_r is the elctrical rotor speed.

By using trigonometric reduction equations, a new matrix is obtained by multiplying the transformation matrix $\left[T_{dq0}\right]$ and above equation

$$\left[T_{dq0}\right]\frac{d}{dt}\left[T_{dq0}\right]^{-1} = \omega_r\begin{bmatrix} 0 & -1 & 0 \\ 1 & 0 & 0 \\ 0 & 0 & 0 \end{bmatrix} \qquad (2.74)$$

Combining equations (2.63), (2.64), (2.70), (2.74), the stator voltage equation (2.71) is written in expanded matrix form:

$$\begin{bmatrix} u_{sd} \\ u_{sq} \\ u_0 \end{bmatrix} = R_s\begin{bmatrix} i_{sd} \\ i_{sq} \\ i_0 \end{bmatrix} + \omega_r\begin{bmatrix} 0 & -1 & 0 \\ 1 & 0 & 0 \\ 0 & 0 & 0 \end{bmatrix}\begin{bmatrix} \psi_{sd} \\ \psi_{sq} \\ \psi_0 \end{bmatrix} + \frac{d}{dt}\begin{bmatrix} \psi_{sd} \\ \psi_{sq} \\ \psi_0 \end{bmatrix} \qquad (2.75)$$

The u_{sd}, u_{sq} can be expressed in equations based on the above matrix:

$$\begin{aligned} u_{sd} &= R_s i_{sd} - \omega_r\psi_{sq} + \frac{d}{dt}\psi_{sd} \\ &= R_s i_{sd} - \omega_r L_{sq}i_{sq} + L_{sd}\frac{d}{dt}i_{sd} \end{aligned} \qquad (2.76)$$

$$\begin{aligned} u_{sq} &= R_s i_{sq} + \omega_r\psi_{sd} + \frac{d}{dt}\psi_{sq} \\ &= R_s i_{sq} + \omega_r L_{sd}i_{sd} + \omega_r\Psi_m + L_{sq}\frac{d}{dt}i_{sq} \end{aligned} \qquad (2.77)$$

The details of derivation of electrical torque T_e are as follows:

The instantaneous input power P to the motor is used, which can be represented as:

$$P = u_a i_a + u_b i_b + u_c i_c \qquad (2.78)$$

After the three-phase voltages and currents are transformed to d-q reference frame, the power can be expressed as:

$$P = \frac{3}{2}(u_{sq} i_{sq} + u_{sd} i_{sd}) \qquad (2.79)$$

where the zero sequence quantities are neglected. The mechanical ouput power P_e is obtained by replacing u_{sq}, u_{sd} as

$$P_e = \frac{3}{2}(\psi_{sd} \omega_r i_{sq} - \psi_{sq} \omega_r i_{sd}) \qquad (2.80)$$

Based on equations (2.36), (2.37), the electrical power can be expressed as:

$$
\begin{aligned}
T_e &= \frac{P_e}{\Omega_r} = \frac{n_p P_e}{\omega_r} = \frac{3 n_p \omega_r}{2 \omega_r}(\psi_{sd} i_{sq} - \psi_{sq} i_{sd}) \\
&= \frac{3 n_p}{2}(L_{sd} i_{sd} i_{sq} + \Psi_m i_{sq} + L_{sq} i_{sq} i_{sd}) \\
&= \frac{3 n_p}{2}((L_{sd} - L_{sq}) i_{sq} i_{sd} + \Psi_m i_{sq})
\end{aligned}
$$

2.3   Controller Design of a PMSM

In the three-phase PMSM control, a more complicated control method, vector control is utilized since all three phases are conducting simultaneously. A sinusoidal wave drive generates less than 1% torque ripple only when both the back-EMF and phase current have sinusoidal waveformes. Because current in each phase is a sinusoidal function of rotor position, separate PWM control for each individual phase current is required, see[6].

Vector control is fundamentally based on two-axis theory. For sinusoidal wave drive motors, the torque is produced by the interaction of the magnetic flux established by permanent magnet and the fundamental ampere-conductor distribution. There are multiple ways to create a two-axis system but generally the method operates with the dq-axis current components, i_{sd} and i_{sq} which may be defined in a variety of reference frames such as rotor or fixed to the stator. Figure 2.3 describes the block diagram of vector control in a PMSM drive system.
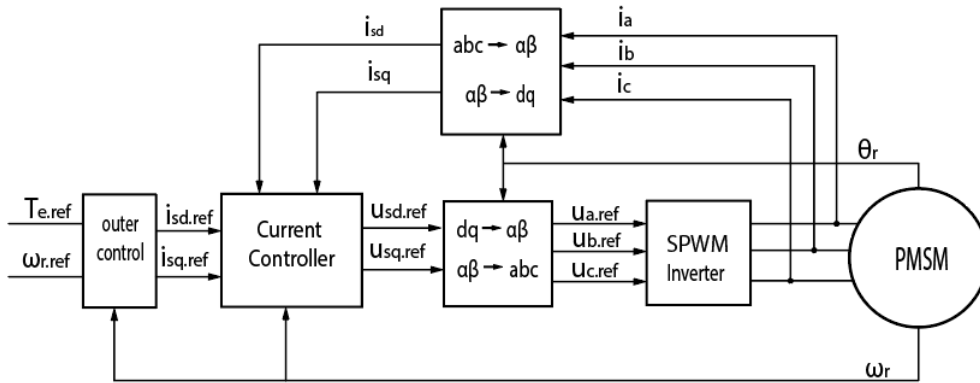
Figure 2.3: Vector Control of a PMSM.

According to [11], FOC(Field Oriented Control) is a crucial variation of vector control. The aim of the FOC method is to control the magnetic field and torque by controlling the stator current component, i_{sd} and i_{sq} or relatively fluxes.

With the information of the stator currents and the rotor position, a FOC technique can control the motor torque and flux in an effective way. The main advantages of this strategy are the fast response and the little torque ripple as mentioned in [8]. FOC relies on field orientation. Once a field-oriented dq reference frame is obtained, the torque is controlled simply by varying the stator current component i_{sq}, and the flux by varying i_{sd}. A conclusion can be drawn from vector control which is an AC motor is forced to behave dynamically as a DC motor by the use of field orientation and feedback control, see[10].

The implementation of FOC will be conducted by using two current regulators, one for the d-axis component, another for the q-axis component. The closed-loop current control is used is to further improve the response time of the current i, to allow precise torque control, and to prevent i from exceeding the maximum value I_{max} in the steady state, while a larger value is allowed at transients sometimes, see[10].

The current regulators should have torque reference and dq current references $i_{sd.ref}, i_{sq.ref}$ as inputs, feed forward of the back-EMF, cross-coupling compensation, active damping and voltage magnitude limitation should be included in order to reduce the control error and improve the performance. The amplitude invariant transformations is used.

The parameters utilized in the controller design are specified below.

Table 2.1: Control parameters

Parameter	Unit	Value	Description
f_s	Hz	10000	Switching frequency
α_c	rad/s	1000	Bandwidth of current regulator
α_ω	rad/s	100	Bandwidth of speed controller
L_{sd}	H	0.00011	Stator inductance in d coordinate
L_{sq}	H	0.00035	Stator inductance in q coordinate
n_p	$--$	4	pole pairs
J	kgm^2	0.019	Inertia of machine
B	Ns/m	0.12	viscous cofficient
Ψ	Wb	0.05	PM magnetic flux linkage
K_{pcd}	$--$	0.11	Proportional constant of d-axis current regulator
K_{icd}	$--$	110	Integral constant of d-axis current regulator
K_{pcq}	$--$	0.35	Proportional constant of q-axis current regulator
K_{icq}	$--$	350	Integral constant of q-axis current regulator
K_{pw}	$--$	1.9	Proportional constant of speed regulator
K_{iw}	$--$	190	Integral constant of speed regulator

In order to control the whole PMSM, the stator voltage needs to be controlled. From the mathematical model of a PMSM section, the stator voltage equations in d-q rotating coordinates are given by:

$$u_{sd} = R_s i_{sd} + L_{sd}\frac{di_{sd}}{dt} - \omega_r L_{sq} i_{sq} \tag{2.81}$$

$$u_{sq} = R_s i_{sq} + L_{sq}\frac{di_{sq}}{dt} + \omega_r L_{sd} i_{sd} + \omega_r \Psi_m \tag{2.82}$$

Moving the terms in relation to ω_r from the RHS to LHS, then terms relating to i_{sd}, i_{sq} are solely on the RHS:

$$u_{sd} + \omega_r L_{sq} i_{sq} = R_s i_{sd} + L_{sd}\frac{di_{sd}}{dt} \tag{2.83}$$

$$u_{sq} - \omega_r L_{sd} i_{sd} - \omega_r \Psi_m = R_s i_{sq} + L_{sq}\frac{di_{sq}}{dt} \tag{2.84}$$

By doing Laplace transformation, the currents in d-q coordinates can be expressed as:

$$i_{sd} = \frac{1}{L_{sd}s + R_s}(u_{sd} + \omega_r L_{sq} i_{sq}) \tag{2.85}$$

$$i_{sq} = \frac{1}{L_{sq}s + R_s}(u_{sq} - \omega_r L_{sd} i_{sd} - \omega_r \Psi_m) \tag{2.86}$$

The transfer function $G_{cd}(s)$ and $G_{cq}(s)$ are defined by:

$$G_{cd}(s) = \frac{1}{L_{sd}s + R_s} \tag{2.87}$$

$$G_{cq}(s) = \frac{1}{L_{sq}s + R_s} \tag{2.88}$$

Note that the equations (2.81) and (2.82) have cross-coupling parts $\omega_r L_{sq} i_{sq}$ and $\omega_r L_{sd} i_{sd}$ respectively. And equation (2.82) has a Back-EMF $\omega_r \Psi_m$. Thus in the following controller design, the cross coupling parts needs to be compensated and feed-forward back-EMF needs to be added.

As shown in Figure 2.4, a complete current control system is designed according to IMC(internal model control).
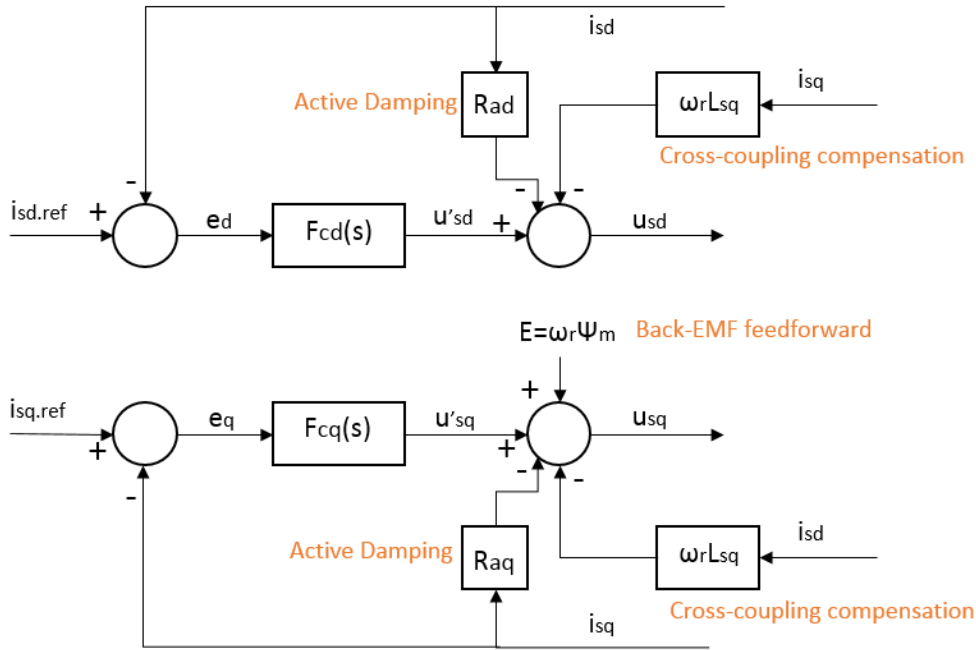

Figure 2.4: View of complete current regulator

As can be shown in Figure 2.4, active damping, cross-coupling compensation, Back-EMF feed forward are included.

In the Figure 2.4, i_{sd}, i_{sq} are measured and are compared to the reference $i_{sd.ref}, i_{sq.ref}$. The error signal $e_d = i_{sd.ref} - i_{sd}, e_q = i_{sq.ref} - i_{sq}$ are the inputs to the current controller. Current controller manipulates the voltage u_{sd}, u_{sq} and thus i_{sd}, i_{sq} can follow $i_{sd.ref}, i_{sq.ref}$ rapidly and accurately. In practice, this manipulation is made using power electronics. In this thesis, assuming the ideal voltage commanded by the current controller can be perfectly generated by the power electronics circuit, see[10].

Based on the equations(2.81) and (2.82), and the information from Figure 2.4, two new equations can be described as:

$$R_s i_{sd} + L_{sd} s i_{sd} - \omega_r L_{sq} i_{sq} = u_{sd} = u'_{sd} - \omega_r L_{sq} i_{sq} - R_{ad} i_{sd} \tag{2.89}$$

$$R_s i_{sq} + L_{sq} s i_{sq} + \omega_r L_{sd} i_{sd} + \omega_r \Psi_m = u_{sq} = u'_{sq} + \omega_r L_{sd} i_{sd} - R_{aq} i_{sq} + \omega_r \Psi_m \quad (2.90)$$

The i_{sd}, i_{sq} can be expressed as in this way:

$$i_{sd} = \frac{1}{L_{sd} s + R_s + R_{ad}} u'_{sd} = G'_{cd}(s) u'_{sd} \quad (2.91)$$

$$i_{sq} = \frac{1}{L_{sq} s + R_s + R_{aq}} u'_{sq} = G'_{cq}(s) u'_{sq} \quad (2.92)$$

The transfer function $G'_{cd}(s)$ and $G'_{cd}(s)$ are defined by:

$$G'_{cd}(s) = \frac{1}{L_{sd} s + R_s + R_{ad}} \quad (2.93)$$

$$G'_{cq}(s) = \frac{1}{L_{sq} s + R_s + R_{aq}} \quad (2.94)$$

2.4 Selection of Controller Parameters

The parameters of the current regulator $F_{cd}(s), F_{cq}(s)$ can be determined according to IMC. From equations (2.93) and (2.94), $G'_{cd}(s), G'_{cq}(s)$ are the transfer functions from u'_{sd}, u'_{sq} to i_{sd}, i_{sq} respectively, which have been illustrated in the Figure 2.5

Figure 2.5 shows the diagram of entire closed-loop system from from i_{ref} to i.
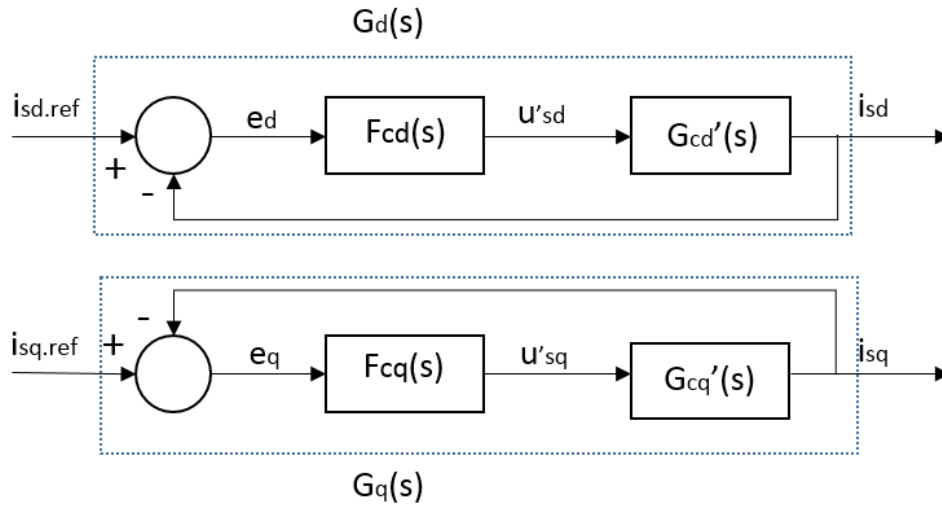
Figure 2.5: Entire closed-loop system from from i_{ref} to i

In the Figure 2.5, $G_d(s), G_q(s)$ are the closed-loop transfer functions from $i_{sd.ref}, i_{sq.ref}$ to i_{sd}, i_{sq} respectively. They can be regarded as the first order low-pass filters. Thus the $G_d(s), G_q(s)$ can be specified as:

$$G_d(s) = \frac{i_{sd}}{i_{sd,ref}} = \frac{\alpha_c}{s + \alpha_c} = \frac{\alpha_c/s}{1 + \alpha_c/s} = \frac{F_{cd}(s) G'_{cd}(s)}{1 + F_{cd}(s) G'_{cd}(s)} \quad (2.95)$$

$$G_q(s) = \frac{i_{sq}}{i_{sq,ref}} = \frac{\alpha_c}{s + \alpha_c} = \frac{\alpha_c/s}{1 + \alpha_c/s} = \frac{F_{cq}(s)G_{cq}^{'}(s)}{1 + F_{cq}(s)G_{cq}^{'}(s)} \tag{2.96}$$

where α_c is the closed-loop system bandwidth.

Based on equations (2.93) and (2.94), the transfer functions $F_{cd}(s), F_{cq}(s)$ can be expressed as:

$$F_{cd}(s) = \frac{\alpha_c}{s}G_{cd}^{'-1}(s) = \frac{\alpha_c}{s}(sL_{sd} + R_s + R_{ad}) \tag{2.97}$$

$$F_{cq}(s) = \frac{\alpha_c}{s}G_{cq}^{'-1}(s) = \frac{\alpha_c}{s}(sL_{sq} + R_s + R_{aq}) \tag{2.98}$$

By transforming transfer functions $F_{cd}(s), F_{cq}(s)$ to PI control form, the new expressions can be described by:

$$F_{cd}(s) = \alpha_c L_{sd} + \frac{\alpha_c(R_s + R_{ad})}{s} = k_{pcd} + \frac{k_{icd}}{s} \tag{2.99}$$

$$F_{cq}(s) = \alpha_c L_{sq} + \frac{\alpha_c(R_s + R_{aq})}{s} = k_{pcq} + \frac{k_{icq}}{s} \tag{2.100}$$

Therefore, the controller parameters $k_{pcd}, k_{pcq}, k_{icd}, k_{icq}$ are:

$$k_{pcd} = \alpha_c L_{sd}, k_{pcq} = \alpha_c L_{sq} \tag{2.101}$$

$$k_{icd} = \alpha_c(R_s + R_{ad}), k_{icq} = \alpha_c(R_s + R_{aq}) \tag{2.102}$$

For the purpose of decreasing the control error, rather than adding more resistance which is highly undesirable due to increased losses, an active resistance is used as shown in 2.4, This technique may also be called "active damping", was proposed in[12].

In order to select "active resistance" R_{ad}, R_{aq}, it is useful to make the $G_{cd}^{'}(s), G_{cq}^{'}(s)$ as fast as as current regulator closed-loop function $G_d(s), G_q(s)$,i.e.,with the same bandwidth α_c. Then, the equations (2.93),(2.93) can be given as:

$$G_{cd}^{'}(s) = \frac{1}{sL_{sd} + R_s + R_{ad}} = \frac{1/L_{sd}}{s + (R_s + R_{ad})/L_{sd}} = \frac{g\alpha_c}{s + \alpha_c} \tag{2.103}$$

$$G_{cq}^{'}(s) = \frac{1}{sL_{sq} + R_s + R_{aq}} = \frac{1/L_{sq}}{s + (R_s + R_{aq})/L_{sd}} = \frac{g\alpha_c}{s + \alpha_c} \tag{2.104}$$

where g is only a gain.

The bandwidth α_c can be expressed as:

$$\alpha_c = \frac{R_s + R_{ad}}{L_{sd}} \tag{2.105}$$

$$\alpha_c = \frac{R_s + R_{ad}}{L_{sq}} \tag{2.106}$$

23

Thus, R_{ad}, R_{aq} can be calculated as:

$$R_{ad} = \alpha_c L_{sd} - R_s \tag{2.107}$$

$$R_{aq} = \alpha_c L_{sq} - R_s \tag{2.108}$$

This in turn yields the controller parameter

$$k_{pcd} = \alpha_c L_{sd}, k_{pcq} = \alpha_c L_{sq} \tag{2.109}$$

$$k_{icd} = \alpha_c^2 L_{sd}, k_{icq} = \alpha_c^2 L_{sq} \tag{2.110}$$

According to [10], this described method gives a current regulator which has two inputs: the control error, and also i_{sd}, i_{sq} directly via the "active resistance".Therefore, it can be called a two-degrees-of-freedom PI controller.

So far, the current control loop is treated as an ideal and linear system. In reality, it is not correct. The terminal voltage u_{sd}, u_{sq} which can be seen from Figure 2.4 have to be limited to an upper and a lower value. The upper value should be V_{max} while the lower value is either 0 or $-V_{max}$. When i_{ref} has a large step, the current controller's output voltage often exceeds V_{max}, especially for higher rotor speed when the back-EMF is large, leading to a large terminal voltage, see[10]. Therefore, the true voltage, reference voltage, is a limitation of the ideal voltage. So the current control loop contains a nonlinearity (saturation) which is used to limit the voltage, as shown in Figure 2.6.

Figure 2.6 shows the PI current controller with voltage saturation and anti-windup loop .
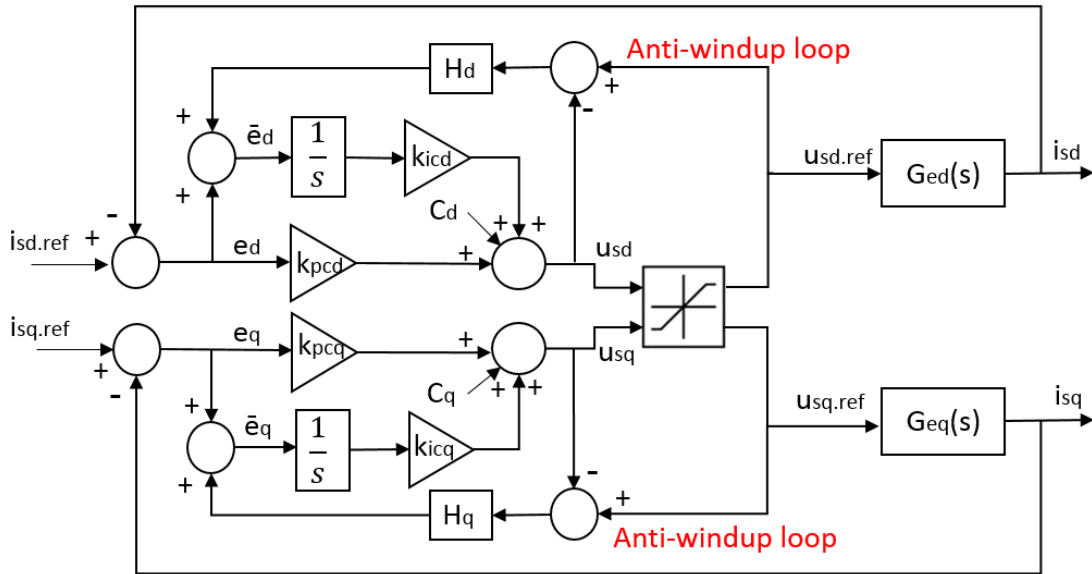

Figure 2.6: PI current controller loop with voltage saturation and anti-windup loop

Additionally, integral term of the PI current controller keeps accumulating the control error during the time of maximum voltage output,, it gets "overcharged". When i starts getting close to i_{ref}, the integrator has wound up so that u remains large. Therefore, i has to shoot over i_{ref} until the windup has been elimated by accumulating of negative control error, see[10].

The solution is to modify the error signal to integrator to limit the integration when the output voltage of the current controller is limited.

As the Figure 2.6 shown, a new error signal to integral term of PI controller is created.

$$\bar{e}_d = (u_{sd.ref} - u_{sd})H_d + e_d \tag{2.111}$$

$$\bar{e}_q = (u_{sq.ref} - u_{sq})H_q + e_q \tag{2.112}$$

The transfer function from $u_{sd.ref}$ to u_{sd} is expressed by:

$$u_{sd} = k_{pcd}e_d + c_d + \frac{k_{icd}}{s}(e_d + H_d(u_{sd.ref} - u_{sd})) \tag{2.113}$$

$$= k_{pcd}e_d + c_d + \frac{k_{icd}}{s}e_d + \frac{k_{icd}}{s}H_d u_{sd.ref} - \frac{k_{icd}}{s}H_d u_{sd} \tag{2.114}$$

By combining like terms, u_{sd} is

$$u_{sd} = \frac{sk_{pcd} + k_{icd}}{s + H_d k_{icd}}e_d + \frac{s}{s + H_d k_{icd}}c_d + \frac{H_d k_{icd}}{s + H_d k_{icd}}u_{sd.ref} \tag{2.115}$$

$u_{sd.ref}$ can be treated as input and e_d and c_d can be regarded as disturbances.

The transfer function from $u_{sq.ref}$ to u_{sq} is expressed by:

$$u_{sq} = k_{pcq}e_d + c_q + \frac{k_{icq}}{s}(e_q + H_q(u_{sq.ref} - u_{sq})) \tag{2.116}$$

$$= k_{pcq}e_q + c_q + \frac{k_{icq}}{s}e_q + \frac{k_{icq}}{s}H_q u_{sq.ref} - \frac{k_{icq}}{s}H_q u_{sq} \tag{2.117}$$

By combining like terms, u_{sq} is

$$u_{sq} = \frac{sk_{pcq} + k_{icq}}{s + H_q k_{icq}}e_q + \frac{s}{s + H_q k_{icq}}c_q + \frac{H_q k_{icq}}{s + H_q k_{icq}}u_{sq.ref} \tag{2.118}$$

Likewise, $u_{sq.ref}$ can be treated as input and e_q and c_q can be regarded as disturbances.

Parameters H_d and H_q are selected as $\frac{1}{k_{pcd}}$ $\frac{1}{k_{pcq}}$:

$$H_d k_{icd} = \frac{k_{icd}}{k_{pcd}} = \frac{\alpha_c^2 L_{sd}}{\alpha_c L_{sd}} = \alpha_c \tag{2.119}$$

$$H_q k_{icq} = \frac{k_{icq}}{k_{pcq}} = \frac{\alpha_c^2 L_{sq}}{\alpha_c L_{sq}} = \alpha_c \tag{2.120}$$

2.5   Speed controller Design

The mechanical dynamics of electric motor drive is given by equation (2.40)

$$J\frac{d\Omega_r}{dt} = T_e - T_L = T_e - B\Omega_r - T_{extra} \tag{2.121}$$

Where J is the total moment of inertia, including the motor itself and mechanical load, see[13]. Ω_r is the mechanical rotor speed, T_e is the electrical driving torque, T_L is the load torque, B is the viscous coefficient. T_{extra} is the extra torque input.

The speed control loop is closed by feedback from the speed reference to the actual speed, as shown in Figure 2.7.
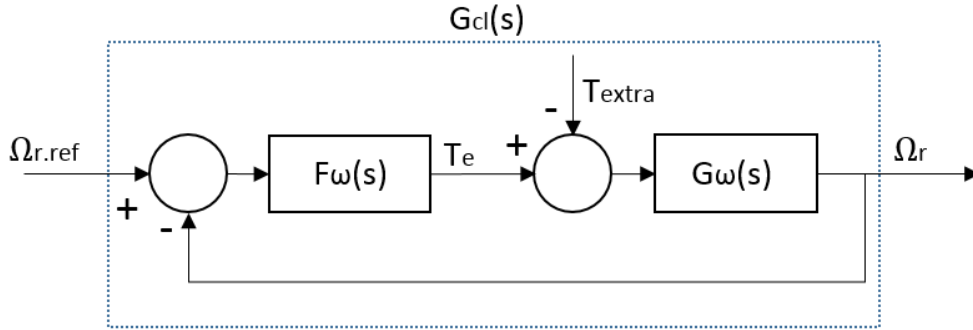

Figure 2.7: Entire speed control loop

By taking the Laplace transform of equation (2.121), the transfer function from T_e-T_{extra} to Ω_r is:

$$G_\omega(s) = \frac{1}{sJ + B} \tag{2.122}$$

The entire transfer function is $G_{cl}(s)$ from the actual speed Ω_r to reference speed $\Omega_{r.ref}$

$$G_{cl}(s) = \frac{\Omega_r}{\Omega_{r.ref}} = \frac{F_\omega(s)G_\omega(s)}{1 + F_\omega(s)G_\omega(s)} = \frac{\alpha_\omega}{s + \alpha_\omega} = \frac{\alpha_\omega/s}{1 + \alpha_\omega/s} \tag{2.123}$$

where α_ω is the speed control bandwidth.

The transfer function $F_\omega(s)$ can be expressed as:

$$F_\omega(s) = \frac{\alpha_\omega}{s}G_\omega(s)^{-1} = \frac{\alpha_\omega}{s}(sJ + B) \tag{2.124}$$

By transforming transfer functions $F_\omega(s)$ to PI control form, the new expressions can be described by:

$$F_\omega(s) = \alpha_\omega J + \frac{\alpha_\omega B}{s} = k_{p\omega} + \frac{k_{i\omega}}{s} \tag{2.125}$$

Therefore, the speed controller parameters $k_{p\omega}, k_{i\omega}$ are:

$$k_{p\omega} = \alpha_\omega J, k_{i\omega} = \alpha_\omega B \qquad (2.126)$$

In the current controller design section, the active damping and anti-windup loop are added to the closed-loop system. Likewise, the speed controller design needs to adopt the active damping and anti-windup loop, as shown in Figure 2.8.
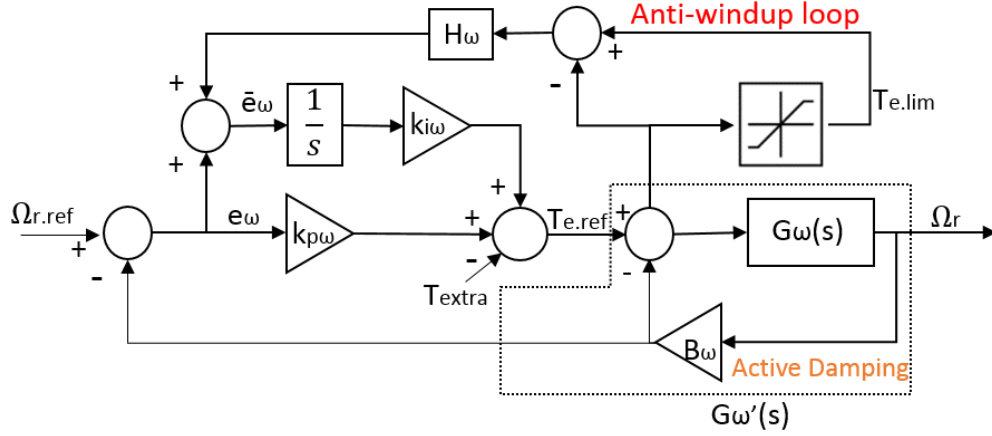

Figure 2.8: Speed control loop with active damping and anti-windup loop

In this case, the transfer function from $T_{e.ref}$ to Ω_r is:

$$G'_\omega(s) = \frac{1}{sJ + B + B_\omega} \qquad (2.127)$$

The proper active damping Ω_r needs to be selected to make the $G'_\omega(s)$ have the same bandwidth as the whole closed-loop transfer function $G_{cl}(s)$.

$$G'_\omega(s) = \frac{1}{sJ + B + B_\omega} = G_{cl}(s) = \frac{g\alpha_\omega}{s + \alpha_\omega} = \frac{1}{\frac{s}{g\alpha_\omega} + \frac{1}{g}} \qquad (2.128)$$

where g is only a gain.

$$g = \frac{1}{B + B_\omega} \qquad (2.129)$$

The active damping can be calculated as

$$B_\omega = \alpha_\omega J - B \qquad (2.130)$$

The transfer function $F_\omega(s)$ needs to be modified to make the entire system have the same bandwidth. The new transfer function $F'_\omega(s)$ can be expressed as:

$$F'_\omega(s) = \frac{\alpha_\omega}{s} G'_\omega(s)^{-1} = \frac{\alpha_\omega}{s}(sJ + B + B_\omega) = \alpha_\omega J + \frac{\alpha_\omega(B + B_\omega)}{s} = k_{p\omega} + \frac{k_{i\omega}}{s} \qquad (2.131)$$

27

Therefore, the new speed controller parameters $k_{p\omega}, k_{i\omega}$ are:

$$k_{p\omega} = \alpha_\omega J, k_{i\omega} = \alpha_\omega(B + B_\omega) \tag{2.132}$$

The same method used in current controller anti-windup design is utilized. As the Figure 2.8 shown, a new error signal to integral term of PI controller is created.

$$\bar{e}_\omega = (T_{e.lim} - T_{e.ref})H_\omega + e_\omega \tag{2.133}$$

The $T_{e.ref}$ is expressed by:

$$T_{e.ref} = k_{p\omega}e_\omega - T_{extra} + \frac{k_{i\omega}}{s}(e_\omega + H_\omega(T_{e.lim} - T_{e.ref})) \tag{2.134}$$

$$= k_{p\omega}e_\omega - T_{extra} + \frac{k_{i\omega}}{s}e_\omega + \frac{k_{i\omega}}{s}H_\omega T_{e.lim} - \frac{k_{i\omega}}{s}H_\omega T_{e.ref} \tag{2.135}$$

By combining like terms, $T_{e.ref}$ is

$$T_{e.ref} = \frac{sk_{p\omega} + k_{i\omega}}{s + H_\omega k_{i\omega}}e_\omega - \frac{s}{s + H_\omega k_{i\omega}}T_{extra} + \frac{H_\omega k_{i\omega}}{s + H_\omega k_{i\omega}}T_{e.lim} \tag{2.136}$$

$T_{e.lim}$ can be treated as input and e_ω and T_{extra} can be regarded as disturbances.

Parameter H_ω is selected as $\frac{1}{k_{p\omega}}$

$$H_\omega k_{i\omega} = \frac{k_{i\omega}}{k_{p\omega}} = \frac{\alpha_\omega^2 J}{\alpha_\omega J} = \alpha_\omega \tag{2.137}$$

2.6 Selection of Current References

Maximum Torque Per Ampere (MTPA) is adopted in the selection of current references. The torque production in a PMSM is a function of $\Psi_m, L_{sd}, L_{sq}, i_{sd}, i_{sq}$ as described in equation (2.39). There are infinite number of i_{sd} and i_{sq} combinations which can generate the same amount of torque.

The torque generation can be separated into two components. The component produced from the permanent magnent flux is called magnetic torque, which can be expressed as:

$$T_{magnetic} = \frac{3n_p}{2}\Psi_m i_{sq} \tag{2.138}$$

The other component produced from rotor saliency is called reluctance torque, which can be expressed as:

$$T_{reluctance} = \frac{3n_p}{2}(L_{sd} - L_{sq})i_{sq}i_{sd} \tag{2.139}$$

In this thesis, a salient PMSM is studied. Normally, inductance along the d-axis is lower than inductance along the q-axis, i.e., L_{sd} is smaller than L_{sq}. (L_{sd} - L_{sq})

is always negative, thus a positive value of i_{sd} would produce a negative reluctance torque, which is opposing the magnetic torque, hence a positive i_{sd} is never desired. Besides, a negative i_{sd} can reduce the required amount of i_{sq} by aiding in the reluctance torque, see[14].

The minimum phase currents can be generated by a particular i_{sd}, i_{sq} for any torque level. It is similar to maximizing the torque output for a specific amount of current. Thus, the operation principle is called Maximum Torque per Ampere(MTPA).

By introducing the current angle β, and stator current I_s, the i_{sd}, i_{sq} can be expressed by:

$$i_{sd} = I_s cos\beta \tag{2.140}$$

$$i_{sq} = I_s sin\beta \tag{2.141}$$

The torque equation (2.39) can be represented by I_s :

$$T_e = \frac{3n_p}{2}(\Psi_m I_s sin\beta + (L_{sd} - L_{sq})I_s^2 sin\beta cos\beta) \tag{2.142}$$

The derivative of torque T_e with respect to current angle β is:

$$\frac{dT_e}{d\beta} = \frac{3n_p}{2}(\Psi_m I_s cos\beta + (L_{sd} - L_{sq})I_s^2 cos2\beta) \tag{2.143}$$

Let the derivative $\frac{dT_e}{d\beta}$ equal to 0, then a fixed current angle β which can generate maximum torque is calculated as:

$$\beta = cos^{-1}(-\frac{\Psi_m}{4(L_{sd} - L_{sq})I_s} - \sqrt{\frac{1}{2} + (\frac{\Psi_m}{4(L_{sd} - L_{sq})I_s})^2}) \tag{2.144}$$

Where I_s could be rated current

Assuming a positive torque request is required, the current magnitude can be calculated as:

$$I_{s.ref} = -\frac{\Psi_m}{2(L_{sd} - L_{sq})cos\beta} + \sqrt{\frac{2}{3n_p(L_{sd} - Lsq)sin\beta cos\beta}T_{e.req} + (\frac{\Psi_m}{2(L_{sd} - L_{sq})cos\beta})^2} \tag{2.145}$$

A limitation to current magnitude needs to added:

$$I_{s.ref.lim} = Lim\{I_{s.ref}\}_0^{Imax} \tag{2.146}$$

Thus the reference current in d-q coordinates can be described as:

$$i_{sd.ref} = I_{s.ref.lim}cos\beta \tag{2.147}$$

$$i_{sq.ref} = I_{s.ref.lim}sin\beta \tag{2.148}$$

3

PWM and Inverter

PWM (Pulse Width Modulation) inverter systems are widely used in a variety of applications as a power-conditioning unit in electric drives, e.g., high voltage DC transmission, active power filters, electric vehicles, alternate energy systems and industrial processes, see[15]. The inverters realize DC-AC power conversion. The DC-input voltage V_{dc} can be obtained from the storage battery in PHEVs.

Inverter fed adjustable speed drives are needed in the PMSM drive system. The switching of inverter plays an significant role in the opertaion of the PMSM drive system, see[16].

In this chapter, the basic principles of PWM are presented in the first place, and after that sinusoidal PWM is illustrated in detail. The three-phase inverter is described after the SPWM is introduced and connections between the SPWM and inverter are also presented, which explains why the reference voltage signal generated from current controller is equal to the average voltage signal established from the inverter.

The parameters utilized in the inverter design are specified below.

Table 3.1: Inverter parameters

Parameter	Unit	Value	Description
V_{batt}	V	330	Battery voltage
R_{batt}	Ohm	0.25	Internal resistance of the battery
C_{dc}	F	$500e-6$	DC capacitance of the converter

3.1 Pulse Width Modulation

According to [16], PWM is a modulation methodology which is based on the pulse duration width. This pulse changes along with the type of modulating signal. On the one hand, the PWM method can be utilized for signal communication or information transfer, on the other hand, it can provide the controller power for major electrical devices particularly to motors. Compared with other available methodologies, the PWM technique has the advantages of less complexity on its implementation and

control, no deviation in temperature and no variation in power due to senescence, see[16].

In order to obtain output AC voltages with the required amplitude and frequency shaped as closely as possible to the sinusoidal wave, a variety of pulse width modulation strategies are used to control the voltage source inverter, see[15].

During the design and implementation of PWM and inverter, the following assumptions are made [17]:

- No voltage drops in valves (diodes, transistors), which means conduction losses are not considered.

- Blanking time is neglected.

- Swithcing losses and off-state losses of inverter are also neglected.

3.2   Sinusoidal PWM

The SPWM (sinusoidal pulse width modulation) technique is one of the most popular PWM techniques due to its benefits of reducing harmonic of inverters. The reason is that three sinusoidal wave are used and displaced as 120° phase difference as reference signals for three phase inverter, see[18].

In this modulation, the modulation signal is a sinusoidal wave and the carrier wave is a triangular wave. The theory is to compare three-phase sinusoidal reference voltages $u_{a.ref}, u_{b.ref}, u_{c.ref}$ established from current controller with carrier wave in order to produce the logical signal, S_a, S_b, S_c. The logical signal can define switching instants of power transistor as mentioned in [19]. A sequence of voltage pulses are acquired by on and off of the power switches based on the given logical signals, which means the logical signals can trigger the respective inverter switches.

Normally, the frequency of carrier wave should be much higher than the frequency of the phase voltages. In this way the phase voltage reference is assumed to be constant during the switching period. The frequency of sinusoidal phase voltage is chosen based on the required inverter output frequency (50/60 Hz).

The constant amplitude pulses with distinct duty cycles in each period is the main characteristic of SPWM technique, see[18]. The width of these pulses vary to gain output voltage control from inverter and the reduction of harmonics, see[20].

The principles of sinusoidal PWM is shown in Figure 3.1, i.e., the comparison between reference voltages and the triangular wave and the generation of logical signal which can determine the switching patterns of inverter.

The logical signal S_a, S_b, S_c are generated by comparison between reference voltages and carrier wave. The switching patterns can be obtained by the equations (3.1),(3.2),(3.3).
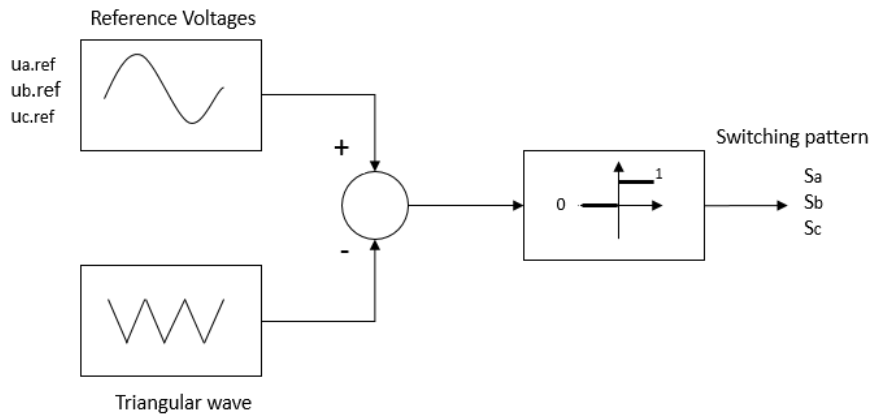
Figure 3.1: Sinusoidal PWM

$$S_a = \begin{cases} 1 & if \ u_{a.ref} \geq triangular \ wave \\ 0 & if \ u_{a.ref} < triangular \ wave \end{cases} \tag{3.1}$$

$$S_b = \begin{cases} 1 & if \ u_{b.ref} \geq triangular \ wave \\ 0 & if \ u_{b.ref} < triangular \ wave \end{cases} \tag{3.2}$$

$$S_c = \begin{cases} 1 & if \ u_{c.ref} \geq triangular \ wave \\ 0 & if \ u_{c.ref} < triangular \ wave \end{cases} \tag{3.3}$$

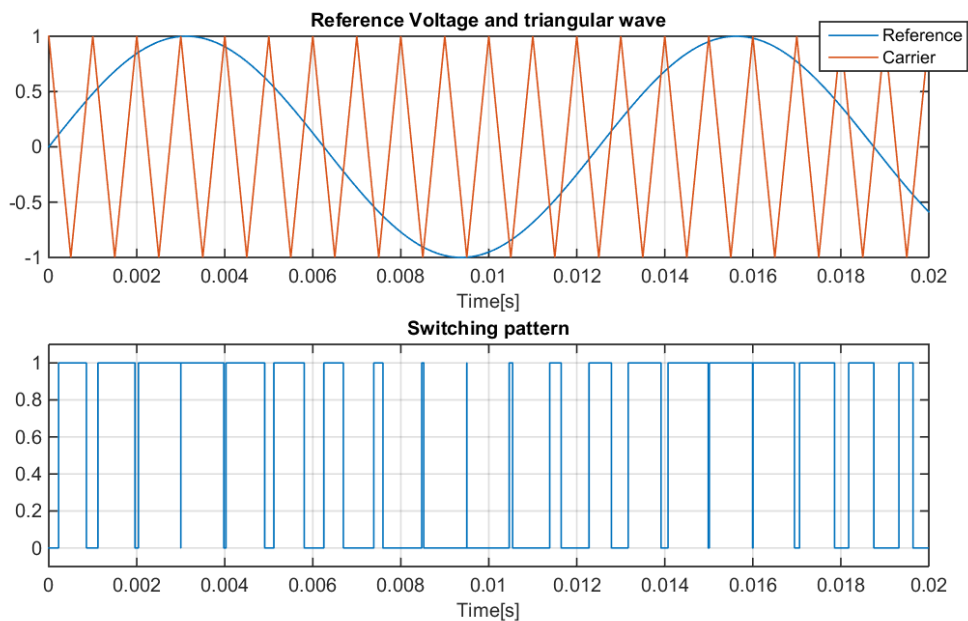Figure 3.2 shows the conventional SPWM signal generation technique for three phase inverter.

Figure 3.2: Sinusoidal PWM basic waveforms

3.2.1 Mathematical Implementation

It is well-known that the the value of a duty cycle should be between 0 and 1. The maximum sinusoidal phase voltage is $\frac{V_{dc}}{2}$. The duty cycles d_a, d_b, d_c can be calculated from the phase voltage references $u_{a.ref}, u_{b.ref}, u_{c.ref}$ and the DC-link voltage V_{dc} as

$$d_a = 0.5 + \frac{u_{a.ref}}{V_{dc}} \tag{3.4}$$

$$d_b = 0.5 + \frac{u_{b.ref}}{V_{dc}} \tag{3.5}$$

$$d_c = 0.5 + \frac{u_{c.ref}}{V_{dc}} \tag{3.6}$$

It is apparent that the values of duty cycles d_a, d_b, d_c are between 0 and 1. The logical signals S_a, S_b, S_c can be obtained by comparing duty cycles and the carrier wave.

$$S_a = \begin{cases} 1 & if \ d_a \geq carrier \ wave \\ 0 & if \ d_a < carrier \ wave \end{cases} \tag{3.7}$$

$$S_a = \begin{cases} 1 & if \ d_b \geq carrier \ wave \\ 0 & if \ d_b < carrier \ wave \end{cases} \tag{3.8}$$

$$S_a = \begin{cases} 1 & if \ d_c \geq carrier \ wave \\ 0 & if \ d_c < carrier \ wave \end{cases} \tag{3.9}$$

In this case, the carrier wave is a triangular wave between 0 and 1. The width of the pulses S_a, S_b, S_c can be varied by changing the duty cycle of PWM.

3.3 Inverter

The VSI (voltage source inverter) has a DC input voltage V_{dc} obtained from battery. The magnitude of this DC input voltage is usually constant. The inverter is to utilize this DC input voltage and reference voltage to produce AC output voltage, where the magnitude and frequency can be controlled, see[18].

The voltage and current are controlled with 120° different in each phase. According to [15], the controlling signals of three-phase PWM inverters have many switching patterns. The operations of three-phase inverter can be defined in eight modes which shows status of each switch in each operation mode.

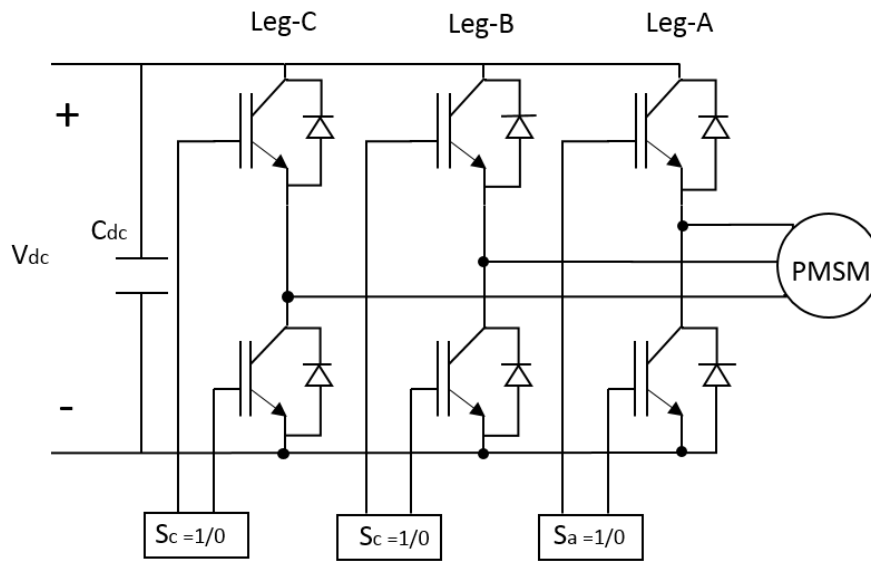Figure 3.3 shows a block diagram of three-phase inverter

Figure 3.3: Three-phase inverter

For the purpose of avoiding undefined switching states and undefined AC output line voltages in the inverter, the switches of any leg of the inverter cannot be switched off simultaneously, see[18].

According to the Figure 3.3, three legs have six switches. Each leg has a top switch and a lower switch. The top switch and lower switch cannot be on or off simultaneously. Thus each leg has two states, top switch on, lower switch off or top switch off, lower switch on. Three legs therefore have eight operation modes.

The status of switches of each leg can be determined by the switching states S_a, S_b, S_c. For leg A, the $S_a = 1$ means top switch on, lower switch off, conversely, $S_a = 0$ means top switch off, lower switch on. Similary, for leg B, the $S_b = 1$ means top switch on, lower switch off, conversely, $S_b = 0$ means top switch off, lower switch on. For leg C, $S_c = 1$ means top switch on, lower switch off, conversely, $S_c = 0$ means top switch off, lower switch on.

Since the switching states S_a, S_b, S_c always will be either 0 or 1, either the top switch or the lower switch will be on. Thus the inverter can be simplified by changing the electronic switches to "mechanical switches", as shown in Figure 3.4.

Figure 3.4 shows the simplified three-phase inverter with three-phase RL circuit.
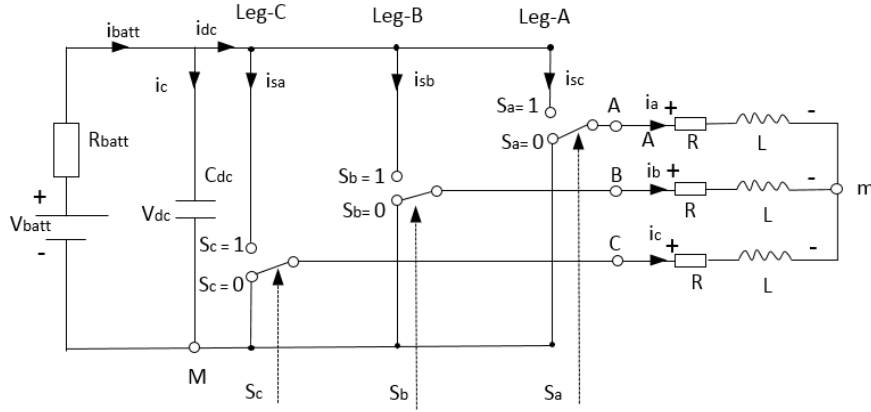
35

Figure 3.4: simplified three-phase inverter with three-phase RL circuit

The derivation of phase voltages is as follows :

Based on Figure 3.4, from point A to point m, the A phase voltage is

$$u_a = V_{Am} = Ri_a + L\frac{di_a}{dt} + e_a \tag{3.10}$$

where e_a is the back-EMF of phase A

$$u_b = V_{Bm} = Ri_b + L\frac{di_b}{dt} + e_b \tag{3.11}$$

where e_b is the back-EMF of phase B

$$u_c = V_{Cm} = Ri_c + L\frac{di_c}{dt} + e_c \tag{3.12}$$

where e_c is the back-EMF of phase C

The sum of V_{Am}, V_{Bm}, V_{Cm} is

$$V_{Am} + V_{Bm} + V_{Cm} = R(i_a + i_b + i_c) + L_c\frac{d(i_a + i_b i_c)}{dt} + (e_a + e_b + e_c) \tag{3.13}$$

where $i_a + i_b + i_c = 0$, assuming the back-EMF is without zero sequence, thus $e_a + e_b + e_c$ is equal to 0.

Hence,

$$V_{Am} + V_{Bm} + V_{Cm} = 0 \tag{3.14}$$

The voltages from from point A, B, C to point M are

$$V_{AM} = V_{Am} + V_{mM} \tag{3.15}$$

$$V_{BM} = V_{Bm} + V_{nM} \tag{3.16}$$

$$V_{CM} = V_{Bm} + V_{nM} \tag{3.17}$$

The sum of V_{AM}, V_{BM}, V_{CM} is

$$V_{AM} + V_{BM} + V_{CM} = (V_{Am} + V_{Bm} + V_{Cm}) + 3V_{mM} \tag{3.18}$$

Due to $V_{Am} + V_{Bm} + V_{Cm} = 0$, the V_{mM} is

$$V_{mM} = \frac{V_{AM} + V_{BM} + V_{CM}}{3} \tag{3.19}$$

Therefore the phase voltages u_a, u_b, u_c can be expressed as:

$$u_a = V_{Am} = V_{AM} - V_{mM} = V_{AM} - \frac{V_{AM} + V_{BM} + V_{CM}}{3} = \frac{2}{3}V_{AM} - \frac{1}{3}(V_{BM} + V_{CM}) \tag{3.20}$$

$$u_b = V_{Bm} = V_{BM} - V_{mM} = V_{BM} - \frac{V_{AM} + V_{BM} + V_{CM}}{3} = \frac{2}{3}V_{BM} - \frac{1}{3}(V_{AM} + V_{CM}) \tag{3.21}$$

$$u_c = V_{Cm} = V_{CM} - V_{mM} = V_{CM} - \frac{V_{AM} + V_{BM} + V_{CM}}{3} = \frac{2}{3}V_{CM} - \frac{1}{3}(V_{AM} + V_{BM}) \tag{3.22}$$

The average of V_{AM} can be expressed by the DC-link voltage V_{dc} and duty cycle d_a:

$$V_{AM.avg} = \frac{1}{T} \int_0^T V_{AM}dt = V_{dc}d_a \tag{3.23}$$

Similarly, V_{BM}, V_{CM} can be expressed as:

$$V_{BM.avg} = \frac{1}{T} \int_0^T V_{BM}dt = V_{dc}d_b \tag{3.24}$$

$$V_{CM.avg} = \frac{1}{T} \int_0^T V_{CM}dt = V_{dc}d_c \tag{3.25}$$

The average of V_{nM} is

$$V_{mM.avg} = \frac{1}{T} \int_0^{T_s} V_{mM}dt = \frac{1}{T} \int_0^T \frac{V_{AM} + V_{BM} + V_{CM}}{3}dt = \frac{V_{dc}}{3}(d_a + d_b + d_c) \tag{3.26}$$

Therefore the average phase voltage can be expressed as:

$$u_{a.avg} = V_{Am.avg} = V_{AM.avg} - V_{mM.avg} = V_{dc}d_a - \frac{V_{dc}}{3}(d_a + d_b + d_c) \tag{3.27}$$

$$u_{b.avg} = V_{Bm.avg} = V_{BM.avg} - V_{mM.avg} = V_{dc}d_b - \frac{V_{dc}}{3}(d_a + d_b + d_c) \tag{3.28}$$

$$u_{c.avg} = V_{Cm.avg} = V_{CM.avg} - V_{mM.avg} = V_{dc}d_c - \frac{V_{dc}}{3}(d_a + d_b + d_c) \tag{3.29}$$

Based on the duty cycle equations (3.4),(3.5),(3.6), the average phase voltage can be further written as

$$u_{a.avg} = V_{dc}d_a - \frac{V_{dc}}{3}(d_a + d_b + d_c) = 0.5V_{dc} + u_{a.ref} - 0.5V_{dc} - \frac{u_{a.ref} + u_{a.ref} + u_{a.ref}}{3} \tag{3.30}$$

$$u_{b.avg} = V_{dc}d_b - \frac{V_{dc}}{3}(d_a + d_b + d_c) = 0.5V_{dc} + u_{b.ref} - 0.5V_{dc} - \frac{u_{a.ref} + u_{a.ref} + u_{a.ref}}{3} \tag{3.31}$$

$$u_{c.avg} = V_{dc}d_c - \frac{V_{dc}}{3}(d_a + d_b + d_c) = 0.5V_{dc} + u_{c.ref} - 0.5V_{dc} - \frac{u_{a.ref} + u_{a.ref} + u_{a.ref}}{3} \tag{3.32}$$

Becasue $u_{a.ref} + u_{a.ref} + u_{a.ref}$ is equal to zero, the phase voltages are:

$$u_{a.avg} = u_{a.ref} \tag{3.33}$$

$$u_{b.avg} = u_{a.ref} \tag{3.34}$$

$$u_{c.avg} = u_{a.ref} \tag{3.35}$$

It shows that the reference voltage signal generated from current controller is equal to the average voltage signal established from the inverter.

From the Figure 3.4, the battery is assumed as a fixed voltage, V_{batt}, the R_{batt} is the resistance. For the DC-link capacitor,

$$C_{dc}\frac{dV_{dc}}{dt} = i_c = i_{batt} - i_{dc} \tag{3.36}$$

$$i_{batt} = \frac{V_{batt} - V_{dc}}{R_{batt}} \tag{3.37}$$

Therefore,

$$C_{dc}\frac{dV_{dc}}{dt} = \frac{V_{batt} - V_{dc}}{R_{batt}} - i_{dc} \tag{3.38}$$

Taking the Laplace transform, then the DC-link voltage can be expressed as:

$$V_{dc} = \left(\frac{V_{batt} - V_{dc}}{R_{batt}} - i_{dc}\right)\frac{1}{C_{dc}}\frac{1}{s} \tag{3.39}$$

The DC-link current i_{dc} is expressed as:

$$i_{dc} = i_{sa} + i_{sa} + i_{sa} = S_a i_a + S_b i_b + S_c i_c \tag{3.40}$$

4

Simulation Results and Analysis

In this chapter, for the purpose of verifying the effectiveness of the mathematical model developed and algorithms adopted in the thesis, a number of simulation results are presented. The steady-state characteristics of a PMSM are analyzed. Moreover, the variable-speed drive analysis is carried out. The issues observed during the simulation process are also demonstrated.

Simulation models are implemented in Matlab/Simulink, operating at a sample frequency of 10 kHz.

The motor parameters used in the simulation are given in the table 4.1

Table 4.1: Motor parameters

Parameter	Unit	Value	Description
P_n	W	30000	Rated power
P_{max}	W	75000	Peak power
V_n	V	215	Rated voltage(AC, phase-to-phase)
I_n	A	150	Rated current(RMS)
I_{max}	A	430	Peak current (RMS)
ω_n	RPM	4775	Rated speed
ω_{max}	RPM	13000	Maximum speed
T_n	Nm	60	Rated torque
T_{max}	Nm	175	Peak torque

4.1 Steady-State Characteristics Analysis

According to [21], for assessing the motor performance, the extent to which speed falls when load is applied, and the variation in speed with applied voltage would be the first questions that need to be studied. Steady-state characteristics can indicate how the motor behaves after the transient effects diminish. It is easier to predict and analyze than transient characteristics.

Firstly, the motor with no extra load input is controlled to reach and operate at a steady state, i.e., the rated speed. No extra load means the motor is running without

external torque, the only mechanical resistance is that due to its own friction.

Figure 4.1 shows a variation of the rotor speed with time. The actual rotor speed reaches the reference speed in a short time with speed controller. The reference speed is the rated speed, i.e. the steady-state speed.
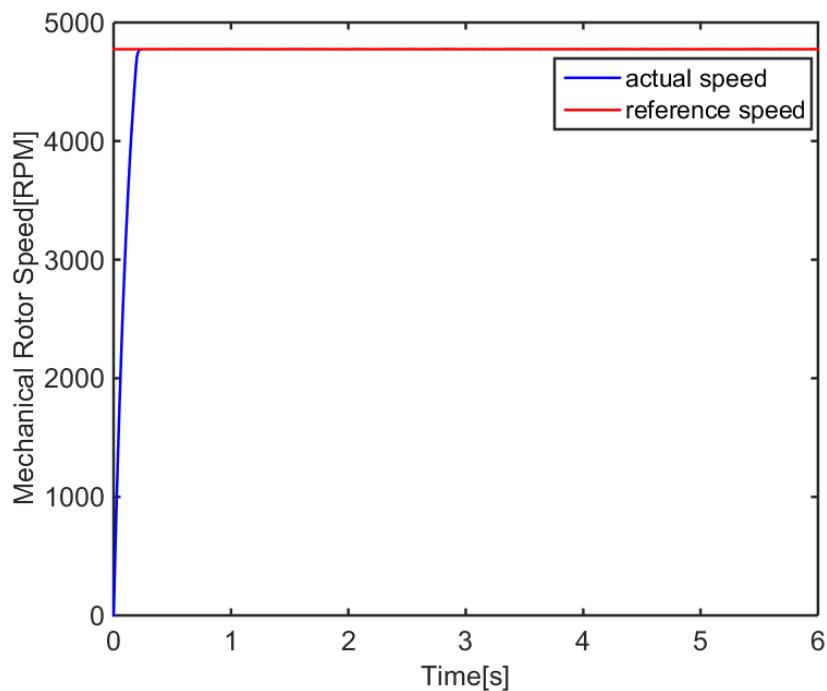

Figure 4.1: Variation of motor speed when tracking the rated speed

Figure 4.2 shows the three-phase currents at the starting and at the steady state. From the Figure 4.2a, it is apparent that the currents are non-sinusoidal and not stable since the motor is attempting to reach the rated speed, see[22]. Figure 4.2b shows the currents become sinusoidal when the motor reaches the rated speed at steady state.

The corresponding dq component of current is given in Figure 4.3. Both d and q axis current are present. It is clear that the i_{sq}, i_{sd} are following the $i_{sq.ref}$ $i_{sd.ref}$ respectively all the time from the beginning to the steady state. The i_{sd} is always negative in order to produce the positive reluctance torque, instead of opposing the magnetic torque.
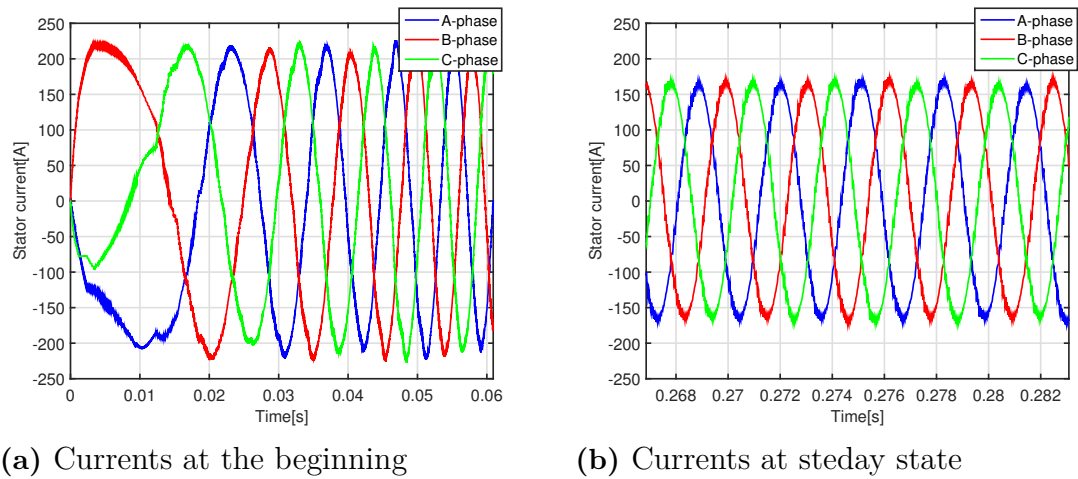
(a) Currents at the beginning

(b) Currents at steday state

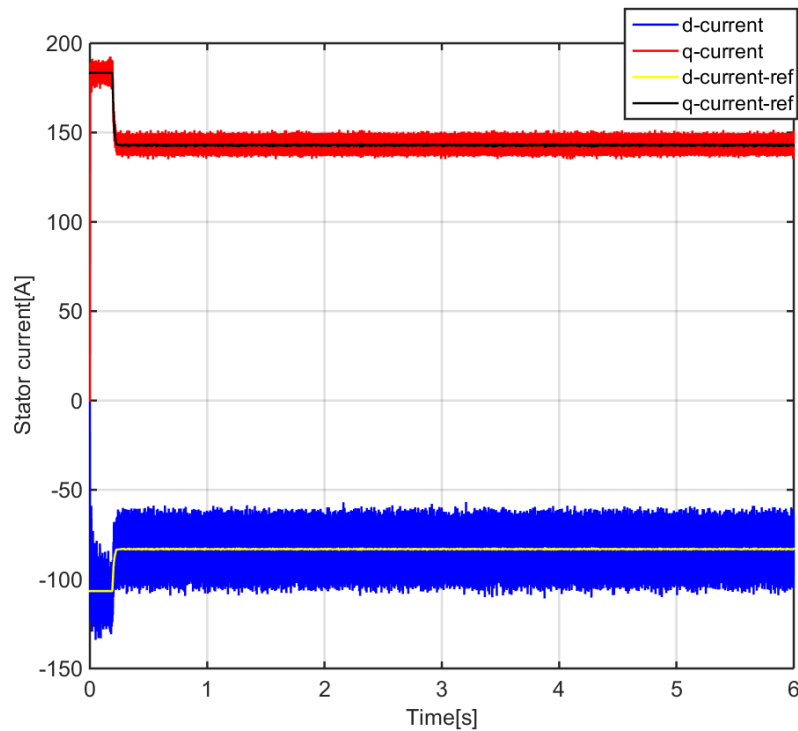**Figure 4.2:** Three-phase currents when tracking the rated speed

Figure 4.3: Stator currents in dq coordinates

Figure 4.4 shows the three-phase voltages at steady state. Figure 4.5 shows electrical torque of the motor and load torque solely produced by its own friction. In order to operate at rated speed, the torque increases rapidly to reach the rated torque 60 Nm. Moreover, it is obvious that the motor torque is equal to the load torque since the motor is running at steady state. The large torque ripple in steady-state operation is one of its main shortcomings.
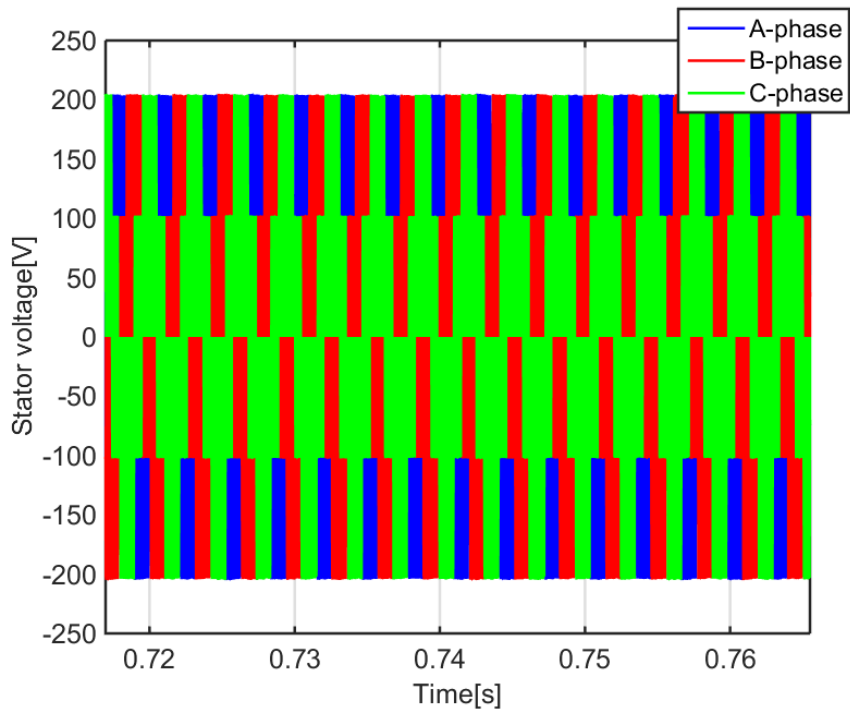
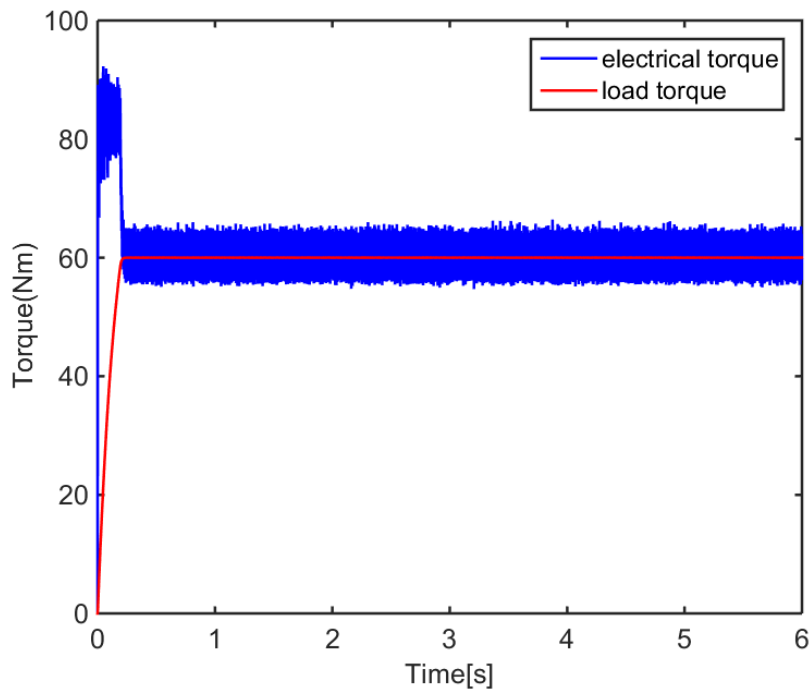**Figure 4.4:** Three-phase voltages at steady state

Figure 4.5: Electrical motor torque and load torque without external torque at steady state

The electrical motor torque is produced based on magnetic flux and the armature

current according to equation 2.39. Load torque is proportional to the product of force and distance. Motor current varies relating to the amount of load torque exerted, see[21]. When the motor is running at steady state, the current is constant, and the motor torque is equal and opposite of the load torque.

Figure 4.5 shows when a motor is accelerating, the motor torque is higher than the load torque. Conversely, when a motor is decelerating, the motor torque is less than the load torque.

When the load on the shaft has been changed, exploring how the speed will vary is a necessity.

Two step changes in load torque were introduced at the second and fourth second starting from 0 Nm to 10 Nm and from 10 Nm to 20 Nm respectively. To achieve the rated speed command of 4775 RPM, motor output torque increased with the application of higher load torque can be seen in Figure 4.6
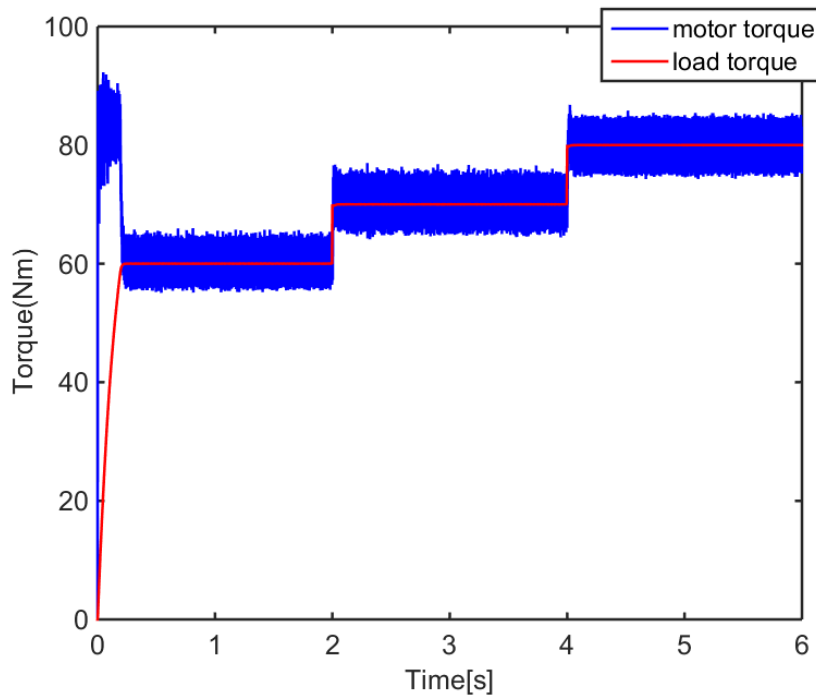

Figure 4.6: Motor torque variation with extra load input when tracking the command speed

Figure 4.7 shows how the speed varies when the rated speed is required. Figure 4.7a shows the view of speed variation during the whole simulation process. The motor speed basically kept constant after the acceleration. When the load torque is applied, the drop in speed is very small which can be seen from Figure 4.7b. It is quite desirable for most application since the only thing to maintain almost constant speed is to set the appropriate armature voltage and keep it constant as mentioned in [21].
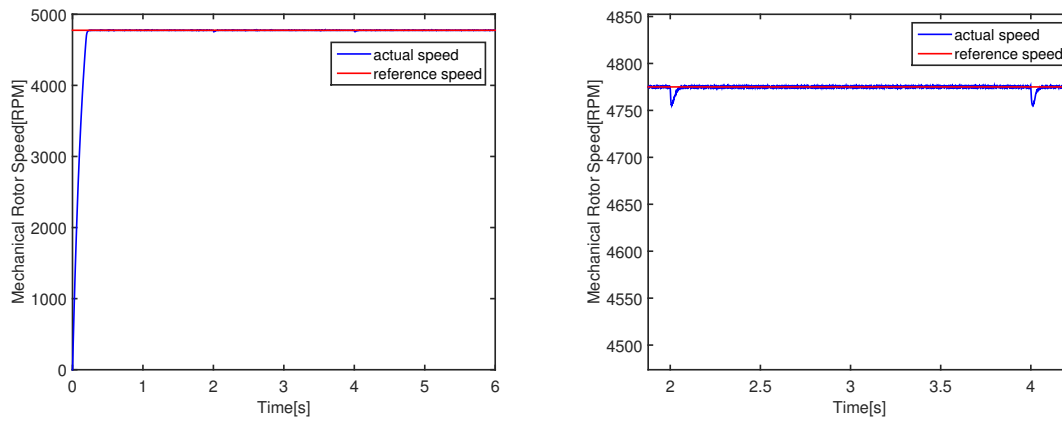
(a) View of speed variation during load variation

(b) View of speed drop when load torque is changed

Figure 4.7: Speed variation during load variation

Figure 4.8 shows the variations of three-phase currents during load variation. It is clear that motor currents vary when the different load torque is applied.
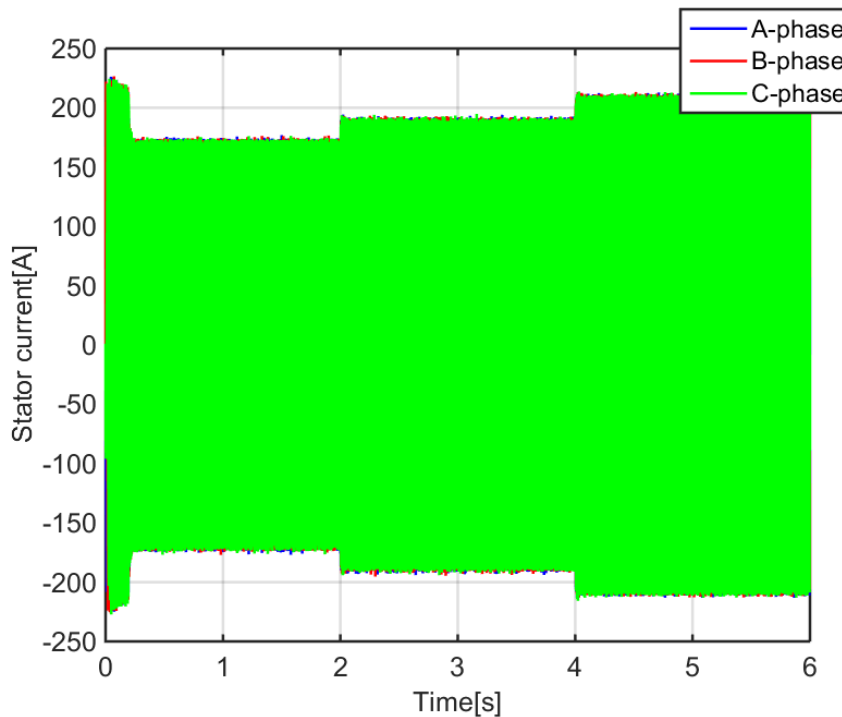

Figure 4.8: Three-phase currents variations during load variation

Figure 4.9 shows the variations of currents i_{sd}, i_{sq} during load variation. The amplitudes of both currents increased with the load torque applied rising. It indicates that the stator currents will go up if the load torque applied to the motor increases.
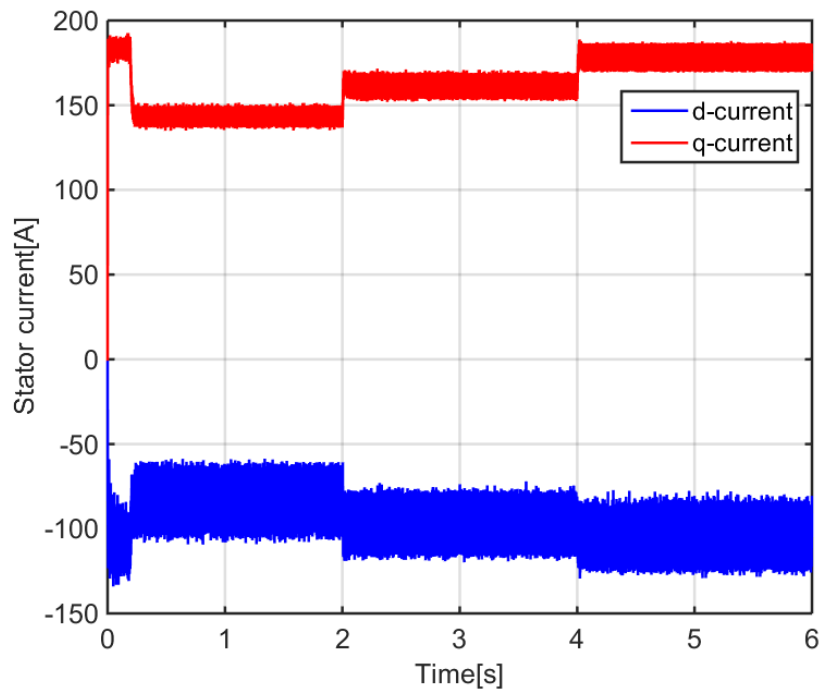
Figure 4.9: Axes currents i_{sd}, i_{sq} variations during load variation at rated speed

From the figures above, regardless of the motor is running without load or with changing load, the rotor speed, electrical torque, currents and voltages can reach the steady state and follow the respective references, which means the system has a good response.

4.2 Variable-Speed Drive Analysis

In this section, the variable-speed drive characteristics are analyzed. A sinusoidal wave is the input speed. This is a simple way to verify if the motor is able to behave nicely in variable-speed scenario.

Figure 4.10 describes the rotor speed response due to sinusoidal input speed reference. The actual speed and reference speed approximately overlap. The system has a good performance when tracking a sinusoidal command speed.

Figure 4.11 shows the actual electric torque and its reference torque. The actual torque and reference torque nearly overlap. It also proves that when the motor tracks the sinudoidal input speed, the electric torque also varies in sinusoidal form..

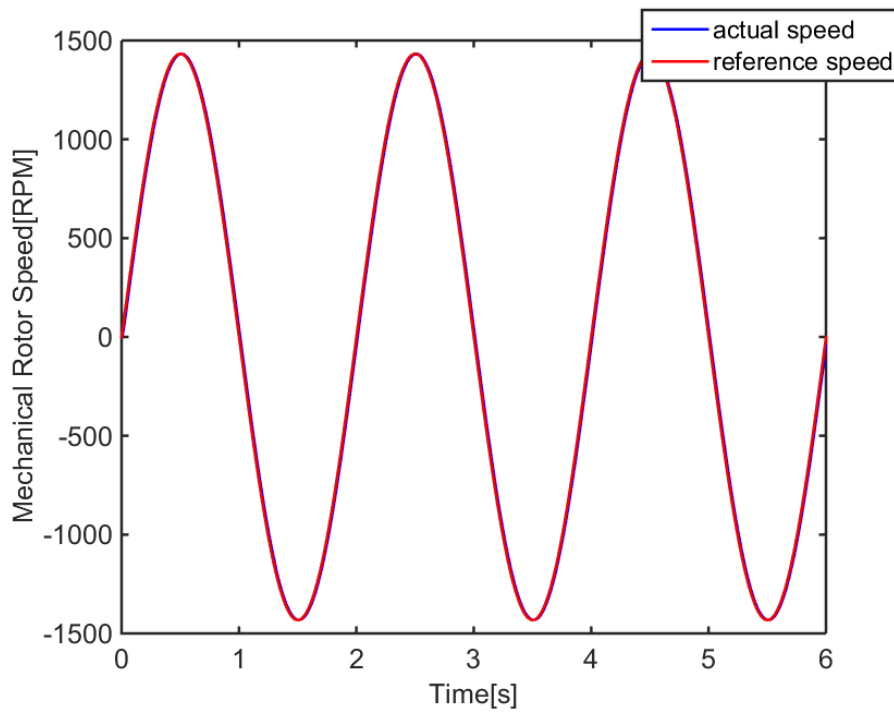**Figure 4.10:** Mechanical rotor speed when tracking the sinusoidal input speed
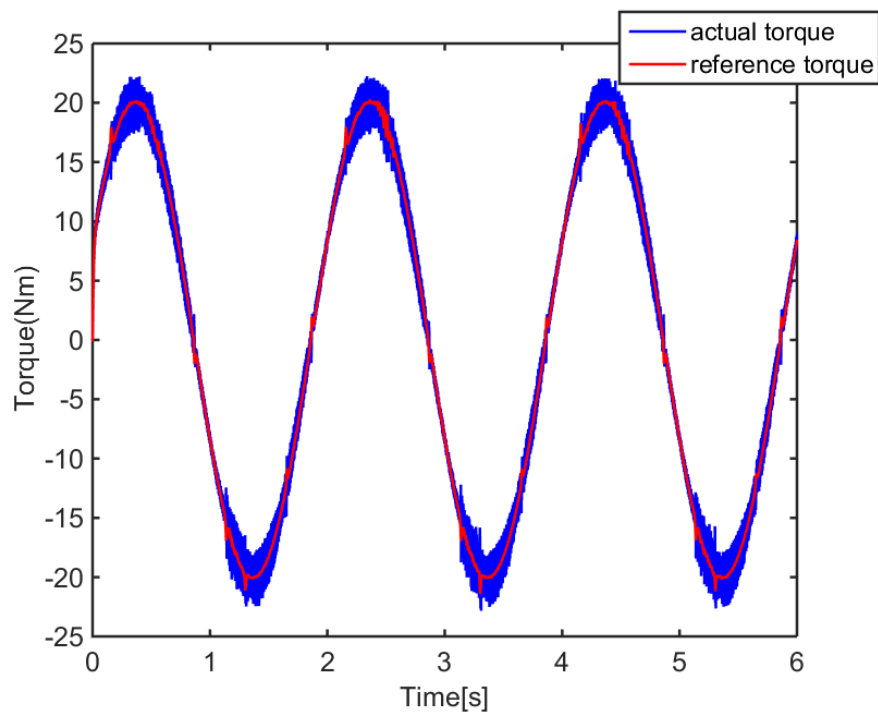
Figure 4.11: Electrical torque when tracking the sinusoidal input speed

Figure 4.12 shows three-phase current variations when tracking the sinusoidal input speed.
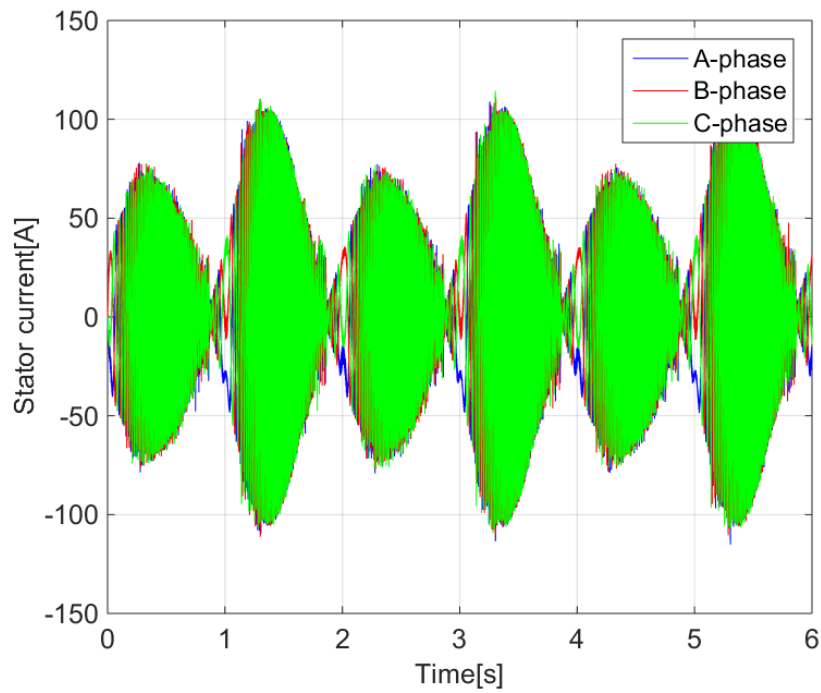
Figure 4.12: Three-phase stator current when tracking the sinusoidal input speed

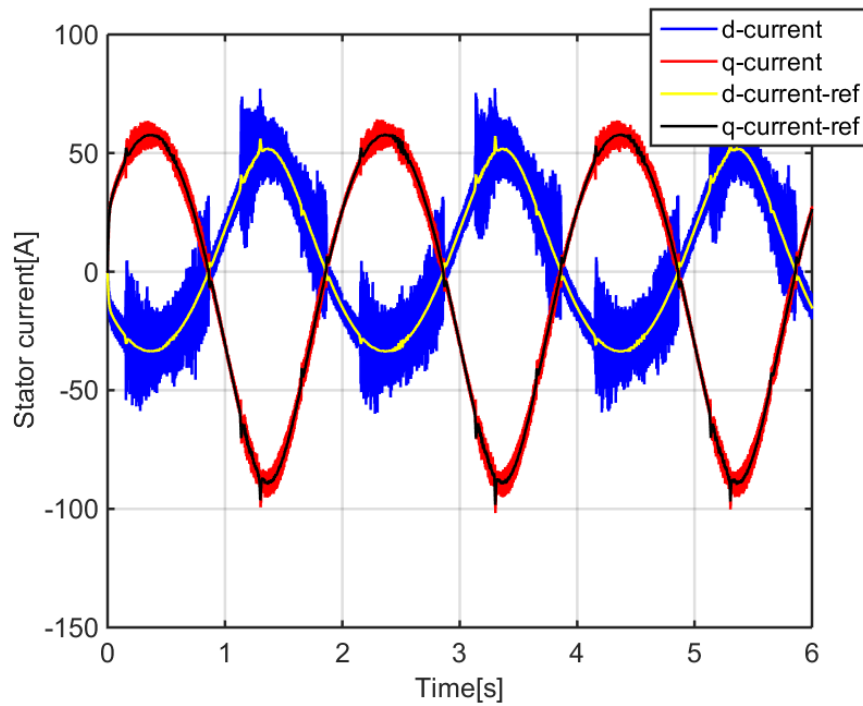Figure 4.13 shows the variations of currents i_{sd}, i_{sq} when tracking the sinusoidal input speed.

Figure 4.13: Axes currents i_{sd}, i_{sq} variations when tracking the sinusoidal input speed

5

PMSM Model Implemented in CarMaker

In this chapter, a brief introduction of CarMaker is conducted. More importantly, how the PMSM plant model and controller are implemented in CarMaker is presented. Relevant results and analysis are also explained in this chapter.

5.1 Overview of CarMaker

According to [23], CarMaker is a simulation software for virtual test driving, specifically for testing passenger cars and light-duty vehicles. Virtual test driving can be used to develop and test the entire vehicle system and entire surrounding environment in the realistic scenarios. A number of models for vehicles, roads, drivers and traffic in CarMaker makes this possible.

CarMaker is a test platform with terrific performance, which guarantees flexibility, productivity and precision for all simulation tasks, thereby it is time-saving and cost-saving for vehicle development. Moreover, another advantage of CarMaker is that it can integrate with external models established from other software like Matlab/Simulink to test the behavior of the various algorithms, see [23].

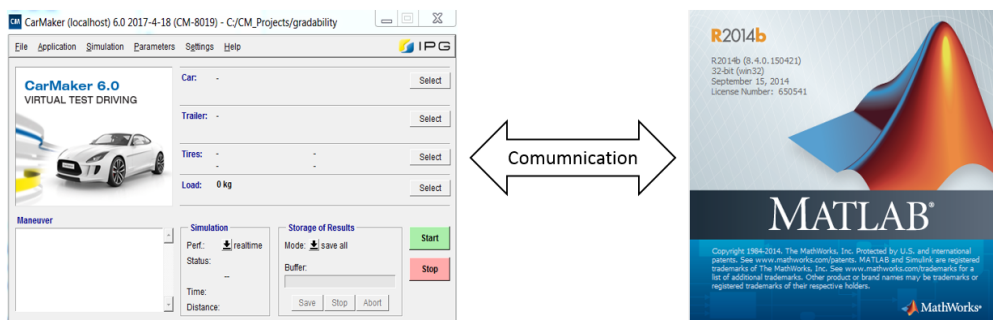Figure 5.1 shows the interface of Matlab and CarMaker, and there is communation between Matlab and CarMaker.

Figure 5.1: Communication between CarMaker and Matlab

5.2 Model Implementation in CarMaker

During the process of model implementation in CarMaker, the Functional Mock-up unit(FMU) is the key part. Some simulation programs or models can be packaged as FMUs in some simulation softwares, like Simulink. The FMU for co-simulation import interface can be imported to CarMaker. Then CarMaker can conduct the test based on the external models or programs.

The FMU interface complies with the Functional Mock-up Interface standard (FMI), which defines an open source standard used to build connections between different simulation programs. According to [24], each FMU includes a zip file containing source code and a XML file with general information of the unit. FMI can enable the integration with any FMI compliant software since it is an international standard and support morn than 70 tools, see [24]

In this thesis project, FMUs of a PMSM plant model and its control unit are exported from Simulink and imported to CarMaker. The interfaces of plant model and control unit of a PMSM in Simulink are shown in Figure 5.2
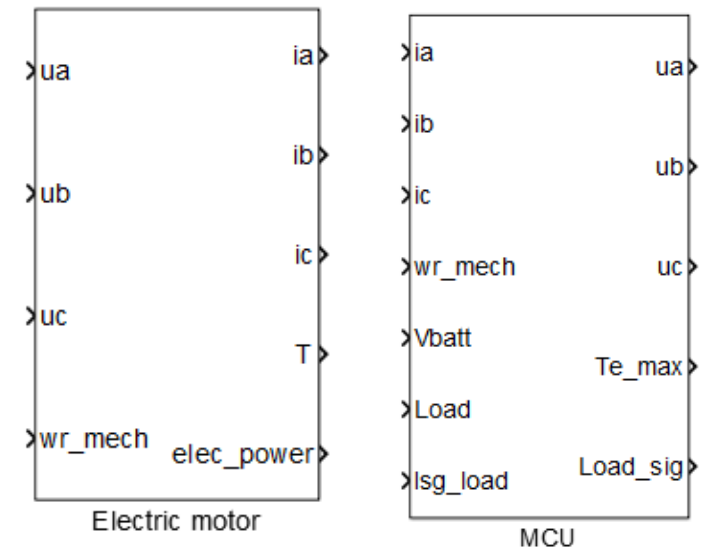
(a) Interface of motor plant model

(b) Interface of motor control unit

Figure 5.2: Interface of motor and controller

Note that the motor control unit consists of current controller, inverter and SPWM. As shown in Figure 5.2a and 5.2b, the three-phase voltage inputs of electric motor are from the three-phase voltages outputs of motor control unit. Three-phase current inputs of control unit are from the three-phase current outputs of electric motor. The signal of mechancial rotor speed ω_{rmech} is from CarMaker, and CarMaker can receive the torque signal(T) from electric motor. The signals of battery and torque request(load) are from CarMaker as well.

Figure 5.3 shows the FMU interface of plant model in CarMaker. Figure 5.4 shows the FMU interface of plant model in CarMaker.

Signal name	Link type	Signal source / destination
☐ FMU Inputs		
➜☐ ua	DDict	FMU.MCU1.Out.ua
➜☐ ub	DDict	FMU.MCU1.Out.ub
➜☐ uc	DDict	FMU.MCU1.Out.uc
➜☐ wr_mech	IF Var	rotv
⊞ FMU Parameter		
☐ FMU Outputs		
☐➜ T	IF Var	Trq
☐➜ elec_power	IF Var	PwrElec
☐➜ ia	DDict	FMU.electricmotor.Out.ia
☐➜ ib	DDict	FMU.electricmotor.Out.ib
☐➜ ic	DDict	FMU.electricmotor.Out.ic

Figure 5.3: FMU interface of a PMSM model in CarMaker

Signal name	Link type	Signal source / destination
☐ FMU Inputs		
➜☐ Isg_load	IF Var	ISGOut.Load
➜☐ Load	IF Var	MotorOut.m0.Load
➜☐ Vbatt	DDict	FMU.battery2.Out.Voltage
➜☐ ia	DDict	FMU.electricmotor.Out.ia
➜☐ ib	DDict	FMU.electricmotor.Out.ib
➜☐ ic	DDict	FMU.electricmotor.Out.ic
➜☐ wr_mech	IF Var	MotorIn.m0.rotv
⊞ FMU Parameter		
☐ FMU Outputs		
☐➜ Load_sig	IF Var	ISGOut.Load
☐➜ Te_max	IF Var	MotorOut.m0.TrqMot_max
☐➜ ua	DDict	FMU.electricmotor.In.ua
☐➜ ub	DDict	FMU.electricmotor.In.ub
☐➜ uc	DDict	FMU.electricmotor.In.uc

Figure 5.4: FMU interface of a PMSM in CarMaker

It is apparent that the FMU inputs and outputs of motor model and its control unit in CarMaker comply with the inputs and outputs of motor model and controller in Simulink.

As a matter of fact, the motor plant model and motor control unit did not function properly in CarMaker, due to the limitations of model, the issues cannot be solved in this thesis and have been put into the future research. However, some reasons which may cause the problem are as follows:

- When the two FMUs, motor plant model and motor control unit were exported from Simulink and loaded back to Simulink for testing, the simulation resulted in an algebraic loop. The algebraic loop is created due to way of two models are connected. Plant model has outputs that are inputs to MCU and MCU outputs are inputs to plant model. Simulink can handle original plant model and control unit in Simulink since it can see what is inside the plant model and control unit. But with FMUs, the Simulink cannot read the way of how the different components connect inside the FMUs. This may lead to the same problem in CarMaker due to the connection of two models.

- Fixed-step solver is used. And the step size must be smaller than the half of switching period of inverter. Otherwise, the carrier wave cannot be produced correctly, which means a smaller step size of plant model and control unit is used in CarMaker. CarMaker cannnot handle this kind of problem based on the simulation results.

6

Conclusions and future work

This chapter includes the conclusions and some proposals for further research.

6.1   Conclusions

This thesis presented the design, implementation and simulation of mathematical model of PMSM and control algorithms for PMSM drives which can be applied to a number of automotive applications.

During the derivation of mathematical model of a PMSM, Clark's and Park's transformations were adopted to transform three-phase coordinates to two-phase(d-q) reference frame. Vector control was used throughout the control design. Current regulator as well as speed controller were designed based on the IMC. The proper calculation of PI-controller parameters ensured correct operation and high precision of controller. Sinusoidal pulse width modulation(SPWM) and inverter were assumed under ideal situations.

The whole PMSM drive system is simulated by the use of Matlab/Simulink. In order to test the PMSM drive system in the entire vehicle in a virtual surrounding environment, CarMaker was used to import FMUs to conduct the test in realistic scenarios. Due to some limitations of the model and CarMaker, the test was not successfully carried out. The possible causes were presented.

Finally, according to the simulation results it is shown that the simulation model has a good performance both in steady state and in variable-speed drive scenario when tracking the command speed, which verifies the PMSM model and control algorithms.

6.2   Future work

Some suggestions for future research in relation to either some issues which were unsolved in the thesis or some ideas that can improve the performance of electric drive system are demonstrated below.

The modulation method can be improved. Sinusoidal pulse width modulation is adopted due to its simplicity and acceptable performances. Experimental tests should be carried out to further verify the simulation results. However, a nicer modulation alternative Space Vector Modulation(SVM) could be utilized and compared with the SPWM. The SVM is well-known for its effectiveness, simple implementation and harmonics reduction.

Regarding the problems of model running in CarMaker, future work could be to adjust the connections of two models to avoid the algebraic loop.

In the design and implementation of SPWM and inverter, no losses were considered and SPWM was regards as in an ideal situation. In fact, the losses and blanking time of inverter need to studied since they are quite important in practice.

That would be fascinating to investigate and test how the motor control unit behaves experimentally[25].

Bibliography

[1] R. Curtin, Y. Shrago, and J. Mikkelsen, "Plug-in hybrid electric vehicles," *Reuters/University of Michigan, Surveys of Consumers*, 2009.

[2] O. Wallmark, "Control of permanent-magnet synchronous machines in automotive applications," Ph.D. dissertation, Chalmers University of Technology, 2006.

[3] S. Chi, "Position-sensorless control of permanent magnet synchronous machines over wide speed range," Ph.D. dissertation, The Ohio State University, 2007.

[4] H. A. Toliyat and S. G. Campbell, *DSP-based electromechanical motion control*. CRC press, 2003.

[5] D. Y. Ohm, "Dynamic model of pm synchronous motors, drivetech," *Inc. Blacksburg, Virginia*, 2000.

[6] S. B. Ozturk, "Modelling, simulation and analysis of low-cost direct torque control of pmsm using hall-effect sensors," Ph.D. dissertation, Texas A&M University, 2007.

[7] J. Luukko *et al.*, "Direct torque control of permanent magnet synchronous machines-analysis and implementation," *Acta Universitatis Lappeenrantaensis*, 2000.

[8] D. Vindel, "Design, simulation and implementation of a pmsm drive system," Master's thesis, Chalmers University of Technology, 2011.

[9] P. Kundur, N. J. Balu, and M. G. Lauby, *Power system stability and control*. McGraw-hill New York, 1994, vol. 7.

[10] L. Harnefors, *Control of variable-speed drives*. Applied Signal Processing and Control, Department of Electronics, Mälardalen University, 2002.

[11] M. Merzoug, F. Naceri *et al.*, "Comparison of field-oriented control and direct torque control for permanent magnet synchronous motor (pmsm)," *World Academy of Science, Engineering and Technology*, vol. 45, pp. 299–304, 2008.

[12] F. B. Del Blanco, M. W. Degner, and R. D. Lorenz, "Dynamic analysis of current regulators for ac motors using complex vectors," *IEEE Transactions on Industry Applications*, vol. 35, no. 6, pp. 1424–1432, 1999.

[13] L. Harnefors, S. E. Saarakkala, and M. Hinkkanen, "Speed control of electrical drives using classical control methods," *IEEE Transactions on Industry Applications*, vol. 49, no. 2, pp. 889–898, 2013.

[14] A. Ahmed, "Maximum torque per ampere (mtpa) control for permanent magnet synchronous machine drive system," Ph.D. dissertation, University of Akron, 2013.

[15] G. Pandian and S. Rama Reddy, "Simulation and implementation of pwm inverter fed induction motor drive," *International Journal of Innovative Research in Science, Engineering and Technology*, vol. 2, no. 11, pp. 6103–13, 2013.

[16] P. Thamizhazhagan and S. Sutha, "Analysis of pwm techniques for power quality improvement in pmsm drives," *Indian Journal of Science and Technology*, vol. 8, no. 24, 2015.

[17] J. Hellsing, *Design and optimization of a permanent magnet motor for a hybrid electric vehicle.* Chalmers University of Technology, 1998.

[18] M. S. Islam, N. I. Raju, and A. U. Ahmed, "Sinusoidal pwm signal generation technique for three phase voltage source inverter with analog circuit & simulation of pwm inverter for standalone load & micro-grid system," *International Journal of Renewable Energy Research (IJRER)*, vol. 3, no. 3, pp. 647–658, 2013.

[19] S. S. Lechat, "Voltage oriented control of three-phase boost pwm converters," Master's thesis, Chalmers University of Technology, 2010.

[20] H. Dehbonei, L. Borle, and C. Nayar, "A review and a proposal for optimal harmonic mitigation in single-phase pulse width modulation," in *Power Electronics and Drive Systems, 2001. Proceedings., 2001 4th IEEE International Conference on*, vol. 1. IEEE, 2001, pp. 408–414.

[21] A. Hughes and B. Drury, *Electric motors and drives: fundamentals, types and applications.* Newnes, 2013.

[22] E. L. C. Arroyo, "Modeling and simulation of permanent magnet synchronous motor drive system," *University of puerto rico, Mayagüez Campus*, 2006.

[23] I. CarMaker, "User's guide version 4.5. 2," *IPG Automotive, Karlsruhe, Germany*, 2014.

[24] S. Rotger-Griful, S. Chatzivasileiadis, R. H. Jacobsen, E. M. Stewart, J. M. Domingo, and M. Wetter, "Hardware-in-the-loop co-simulation of distribution grid for demand response," in *Power Systems Computation Conference (PSCC), 2016.* IEEE, 2016, pp. 1–7.

[25] C. Dubar, "Design and analysis of a fault-tolerant fractional slot pmsm for a vehicle application," Ph.D. dissertation, Chalmers University of Technology, 2016.

A
Appendix 1

A. Appendix 1

II

B

Appendix 2